High-Resolution Mapping of Genome Position Expression Variation in Bacteria
&
Engineering of Microbial Consortia for Cellulosic Biochemical Production

by

Scott A. Scholz

A dissertation submitted in partial fulfillment
of the requirements for the degree of
Doctor of Philosophy
(Cellular and Molecular Biology)
In the University of Michigan
2018

Doctoral Committee:

Assistant Professor Peter Freddolino, Co-Chair
Associate Professor Xiaoxia Nina Lin, Co-Chair
Professor Kenneth Cadigan
Professor Anuj Kumar
Professor Stephen Ragsdale
Professor Thomas Schmidt

Scott A. Scholz

scholz@umich.edu

ORCID iD: 0000-0001-9168-9285

Table of Contents

List of Figures

Abstract

High-resolution mapping of genome position expression variation in bacteria: To elucidate the effect of position in the bacterial genome on gene expression at a high resolution, we have developed a multiplex strategy to construct and analyze a library of genome-integrated reporters in a single mixed population of *Escherichia coli*. By randomly integrating a standardized barcoded reporter with Tn5 transposase, transcription from over 144,000 reporters across the bacterial genome was tracked simultaneously. High-resolution mapping of reporter transcription revealed large peaks of high transcriptional propensity centered on ribosomal RNA operons that have not been previously detected. Genes for amino acid biosynthesis were specifically enriched in high transcriptional propensity regions, while prophages and mobile genetic elements were enriched in low transcriptional propensity regions, demonstrating that the *E. coli* chromosome has evolved gene-independent mechanisms for affecting expression from specific regions. The nucleoid associated proteins H-NS and Fis were highly informative of reporter transcription, which shows ~150-fold variation in transcriptional propensity over its entire length.

Engineering of microbial consortia for cellulosic biochemical production: Consolidated bioprocessing is a potential breakthrough technology for reducing costs of biochemical production from lignocellulosic biomass. Production of cellulase enzymes, saccharification of lignocellulose and conversion of the resulting sugars into a chemical of interest occur simultaneously within a single bioreactor. In this study, synthetic fungal consortia composed of the cellulolytic fungus *Trichoderma reesei* and the production specialist *Rhizopus delemar* demonstrated conversion of microcrystalline cellulose (MCC) and alkaline pre-treated corn stover to fumaric acid in a fully consolidated manner without addition of cellulase enzymes or expensive supplements such as yeast extract. A Titer of 6.87 g/L of fumaric acid, representing 0.17 w/w yield, were produced from 40 g/L MCC with a productivity of 31.8 mg/L/h. In addition, lactic acid was produced from MCC using a fungal consortium with Rhizopus oryzae as the

production specialist. These results are proof-of-concept demonstration of engineering synthetic microbial consortia for CBP production of naturally occurring biomolecules. In order to improve the performance of the fumaric acid production CBP system, we developed selective nitrogen delivery as a method to tune the growth of each specialist. By replacing the urease gene of *T. reesei* with the *amdS* gene from *Aspergillus nidulans,* we reassigned the nitrogen utilization capability of *T. reesei* from urea to acetamide to generate the SND strain. Using SND, we were able to tune the production of fumaric acid in the consortia CBP production system by varying Urea:Acetamid ratio. Tuning enable a higher yield of fumaric acid than previously observed.

Chapter 1 Background and motivation

1.1 Bacterial genome structure and function

The bacterial nucleoid is a dense structure composed of DNA, RNA and proteins that excludes other abundant cellular machinery, such as ribosomes and RNA polymerase (RNAP), from its interior (Chai et al. 2014; Jin and Cabrera 2006; Bakshi, Choi, and Weisshaar 2015). Several studies have demonstrated that packing of the nucleoid is non-random and condition dependent. For example, chromosome conformation capture studies in multiple bacterial species have revealed segments of DNA that preferentially self interact, called chromosome interaction domains (Lioy et al. 2018a; Le et al. 2013a; Marbouty et al. 2015; Wang et al. 2015). During exponential growth, RNAPs are also organized into tight foci on the nucleoid surface, actively transcribing the ribosomal RNA operons (*rrn*) (Cabrera and Jin 2006a), most of which appear spatially co-localized (Gaal et al. 2016). Despite the specific localization of DNA and RNAP, previous findings based on site-specific integrations have suggested that gene expression from different genomic loci is roughly equivalent, except for the effect of gene dosage, which decreases from the origin of replication to the terminus during exponential growth (Beckwith, Signer, and Epstein 1966; Sousa, de Lorenzo, and Cebolla 1997; Schmid and Roth 1987). Higher gene dosage near the origin is a result of multiple replication initiation events before terminus replication and cell division (Cooper and Helmstetter 1968); historically, the bacterial chromosome has otherwise been considered universally accessible structurally and for transcription (Masters 1977).

By measuring GFP fluorescence from a terminator-flanked reporter integrated into several sites, Block et al. demonstrated that gene expression variation from the origin to the terminus corresponded to expected growth-rate dependent gene dosage changes (Block et al. 2012a), consistent with the expectations outlined above. More recently, however, the dogma of uniform expression capability across the genome has been challenged by several lines of evidence. Using a similar approach to Block et al., Bryant et al. demonstrated widely varying expression from a GFP reporter in *E. coli* that did not correlate with genome copy number (Bryant et al. 2014a). Some of the lowest expressing sites were in transcriptionally silent Extended Protein Occupancy Domains (tsEPODs) (Block et al. 2012b; Bryant et al. 2014a; Vora, Hottes, and Tavazoie 2009a), which are regions of high protein occupancy that appear to correlate with low transcript levels. In some cases, the reporter gene expression could be increased by

replacing the tsEPOD with the reporter gene instead of integrating within it (Bryant et al. 2014). For some reporters outside of tsEPODS, expression interference from neighboring genes drove down reporter expression, depending on the relative gene orientation. Gene expression interference between neighboring genes has also been studied in more detail on plasmids within *E. coli* cells (Yeung et al. 2017a). In that study, some of the gene expression interference observed between neighboring genes could be attributed to competition for negative DNA supercoiling and was gene orientation-specific. DNA gyrases and topoisomerases maintain negative supercoiling, which compacts the nucleoid and is important for gene expression (Dorman 2006). Brambilla and Sclavi have also tracked expression of a reporter under a promoter known to be bound by the nucleoid protein H-NS from 9 different sites over the *E. coli* growth period and observed different site-specific expression levels depending on the growth phase (Brambilla and Sclavi 2015).

Despite the specific observations described above, a systematic understanding of the effects of chromosomal position itself on gene expression has so far eluded the field. Previous studies on position-dependent expression variation have been limited to a small number of integration sites, which was appropriate for mechanistic studies into the effects of specific genomic features, but could not reveal the full range of position-dependent effects on transcription. DNA supercoiling, protein occupancy, transcriptional interference and binding of promoters and genes by various nucleoid associated proteins (NAPs) are examples of genomic features that affect expression of large proportions of genes in the bacterial genome. Extensive work has been conducted to characterize the effects of a number of these factors for expression of specific genes. However, genomic features vary simultaneously across the genome, potentially leading to combinatorial effects on gene expression (Martínez-Antonio, Medina-Rivera, and Collado-Vides 2009; Le et al. 2013b). Specific loci may have unique features affecting transcription, which could only be identified by high-resolution mapping of position-dependent expression variation.

Here, we employ Tn5 transposase to perform massively parallel integration of a standardized, barcoded reporter construct to create an empirical map of gene-independent transcriptional propensity across the bacterial genome (Fig. 1). High-resolution transcriptional propensity comparisons with genomic features can reveal both strong and weak correlations with high statistical power. To test the effect of genome position on gene expression, and not native promoter strength, we designed a reporter construct with strong bi-directional terminators (Y.-J. Chen et al. 2013a) and its own inducible promoter (Fig. 1A) . Each reporter construct is tagged with a unique barcode identifier, which allows simultaneous tracking of gene expression from thousands of integrations. Using a modified transposon

footprinting procedure, unique barcodes were paired with integration location, allowing transcribed barcodes to serve as a proxy for the overall abundance of RNA or DNA at each integration address. The σ70 dependent TetO1 promoter drives expression of mNeonGreen (mNG) followed by a 15 base barcode on the 3' UTR of the RNA upon induction by anhydrotetracycline (aTc) (Clavel et al. 2016). The reporter used here was designed to be relatively small in size and have a low transcription rate (Kosuri et al. 2013), in order to minimize the effect of the reporter on the local genome context (Le et al. 2013). The inclusion of an open reading frame on our construct ensures that the transcribed RNA will be subject to typical post-transcriptional phenomena (*e.g.*, co-transcriptional translation and subsequent protection by ribosomes). In keeping with efforts to minimize reporter size, the selection marker is an FRT-flanked kanamycin resistance cassette, and was removed by Flp recombinase before the full-scale profiling procedure (Fig. 1.1A).

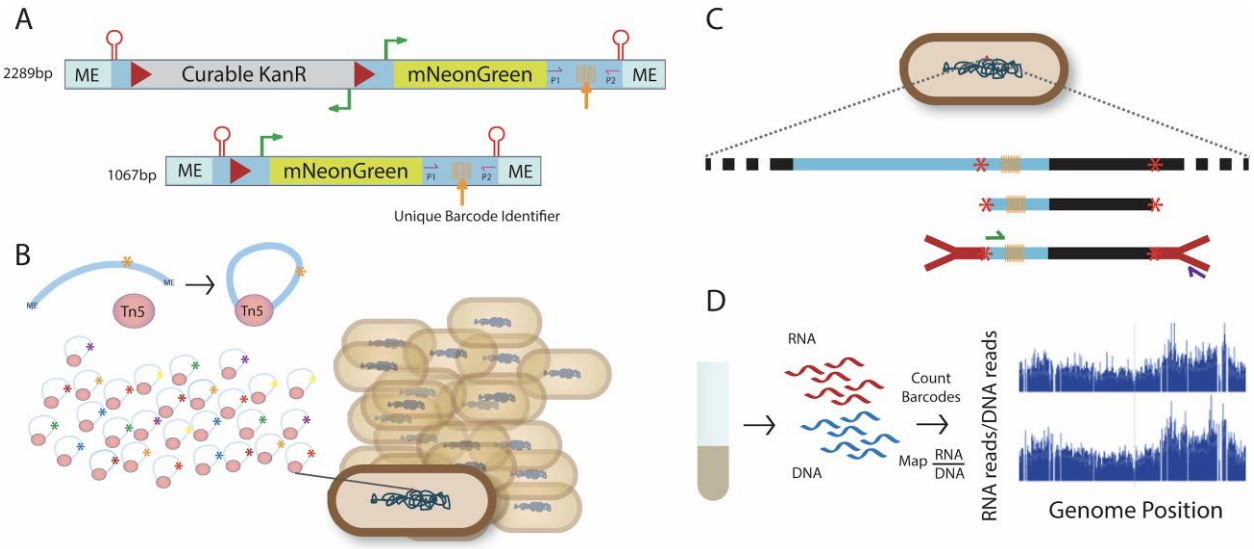

Figure 1.1: Library construction and data acquisition for position-dependent transcriptional propensity mapping. A) mNeonGreen reporter is controlled by the TetO1 promote [cite]. The orange arrow indicates the position of the 15bp barcode that is transcribed with mNG. The construct is flanked by strong bi-directional terminators and mosaic ends (ME), which are recognized by Tn5 transposase. P1 and P2 indicate sites used for light amplification for barcode sequencing. Construct size and features are shown before and after curing of a kanamycin resistance marker (KanR). B) To produce the reporter library, randomly barcoded reporter constructs in complex with Tn5 are electroporated into cells and randomly integrated into the *E. coli* genome in parallel. C) Transposon footprinting pairs barcode sequence (orange) with integration location on the genome (black). 4bp recognition restriction enzymes cut upstream of the barcode and randomly in the downstream genomic DNA. After ligation of the Y-linker (red), construct-containing DNA fragments are specifically amplified and sequenced. D) The reporter library is grown in M9 RDM to OD 0.2. Total RNA and DNA are extracted. After nucleic acid processing (Fig 2.8), the RNA/DNA ratio for each barcode are mapped to their corresponding genomic location.

1.1.1 Nucleoid associated proteins and other factors that affect gene expression

The most abundant NAPs during exponential phase growth, Fis, HU, and HFQ, followed by the paralogs StpA and H-NS, have been studied for their involvement in a variety of processes, depending on the genome context or specific gene (Ali Azam et al. 1999; Dillon and Dorman 2010; Azam and Ishihama 1999; Browning, Grainger, and Busby 2010). Fis is involved in binding to DNA and direct regulation of transcription through a variety of processes (Kahramanoglou et al. 2011a). It can bind to promoter regions of ribosomal RNA and other genes to promote transcription during nutrient rich-conditions, a process which is also sensitive to DNA supercoiling (Newlands et al. 1992). Fis in turn can function to limit the diffusion of DNA supercoiling (Robert Schneider, Travers, and Muskhelishvili 1997). Fis binding can also directly repress genes by blocking RNA polymerase binding, which has been observed specifically at the gyrase promoters (R. Schneider et al. 1999). Because Fis is the most abundant NAP during exponential growth phase and is involved in processes regulating ribosome production and DNA supercoiling, it may play an important role in sensing and responding to physiological state change in the cell (Nilsson et al. 1992; Caramel and Schnetz 2000; Ninnemann, Koch, and Kahmann 1992).

HU is also involved in the regulation DNA supercoiling and allowing bends in DNA to occur more easily (Guo and Adhya 2007; Becker, Kahn, and Maher 2007). Strains without HU display growth and recombination defects and deregulation of genes involved in anaerobic growth and stress response (Oberto et al. 2009; Broyles and Pettijohn 1986). In addition, position specific effects of HU knockout have been demonstrated for the same reporter integrated into different sites around the E. coli genome (Berger et al. 2016). Perhaps it is not surprising that the most abundant NAPs are involved in the essential process of DNA negative supercoiling.

Although highly abundant in the bacterial nucleoid, Hfq is primarily studied in its capacity as a RNA chaperone and involvement in RNA-RNA interactions between small non-coding RNAs and coding RNA. Hfq is not specifically localized to the nucleoid as specifically as other proteins considered NAPs and may primarily be a part of the nucleoid through its contacts with RNA (Ali Azam et al. 1999). However, Hfq can bind directly to DNA and may have undiscovered or underappreciated roles in genome organization (Takada et al. 1997; Jiang et al. 2015).

H-NS is the major nucleoid associated protein responsible for gene silencing. H-NS can bind DNA in a sequence specific manner or in a relatively sequence independent manner, oligmerizing along mainly AT-rich DNA sequences (Kahramanoglou et al. 2011a). Some groups have proposed that H-NS may also constrain negative supercoiling in DNA (Tupper et al. 1994). However, this role is independent of H-NS silencing activity in some cases (Atlung and Ingmer 1997; Ueguchi and Mizuno 1993). In addition

to intrinsic H-NS binding preferences, Hha, YdgT, H-NS paralog StpA and perhaps other factors can also influence H-NS binding to DNA (Madrid et al. 2007; Ueda et al. 2013). StpA can heterodimerize with H-NS and has overlapping DNA binding site preferences in WT cells (Uyar et al. 2009a). However, StpA can only bind to a subset of sites on DNA shared with H-NS in H-NS mutant strains. StpA also has RNA chaperone activity and promotes annealing through simultaneous binding of two RNAs (Mayer et al. 2007). It has also been shown to promote splicing in vivo of a td group I intron (Waldsich 2002). NAPs with general binding to DNA are due in part to electrostatic interactions with the DNA backbone (Gao et al. 2017a). This interaction mode may contribute the the blurred lines between NAP, transcription factor and RNA binding protein.

DNA supercoiling, protein occupancy, transcriptional interference and binding of promoters and genes by various Nucleoid Associated Proteins (NAPs) are examples of genomic features that affect expression of large proportions of genes in the bacterial genome. Extensive work has been conducted to characterize the effects of a number of these factors for expression of specific genes. However, genomic features vary simultaneously across the genome, potentially leading to unpredictable combinatorial effects on gene expression (Martínez-Antonio, Medina-Rivera, and Collado-Vides 2009b; T. B. K. Le et al. 2013b). Specific genetic elements may have unknown effects, which could only be identified by high-resolution mapping of position-dependent expression variation.

1.2 Microbial consortia-based consolidated bioprocessing of lignocellulosic biomass

1.2.1 Development of productive microbial consortia

Lignocellulosic biomass is an attractive substrate for bioconversion into industrial chemicals because it is the most abundant renewable bio-feedstock on earth. As a non-edible plant substrate, lignocellulose can be produced as agricultural and forest residues, which do not require massive land use changes. There are also strong social motivations for using lignocellulosic biomass as a replacement for edible substrates currently used for industrial bioconversions, such as corn and simple sugars (Dunn et al. 2013). However, due to the recalcitrant nature of lignocellulose to enzymatic hydrolysis, it has not been widely used as an industrial feedstock (Carroll and Somerville 2009). Consolidated bioprocessing (CBP) has been widely discussed as a strategy for improving the efficiency of converting lignocellulosic biomass into industrial biochemical (Liao et al. 2016; Parisutham, Kim, and Lee 2014; Brethauer and Studer 2014a; Kawaguchi et al. 2016) . In CBP enzyme production, enzymatic hydrolysis and conversion of resulting sugars to biochemicals occur simultaneously in a single reaction vessel, resulting in

significant potential cost savings (Olson et al. 2012). One approach for CBP has been to genetically engineer one microorganism to produce cellulases and convert sugars into desired biochemicals. Indeed, efficient ethanol production has been demonstrated using this approach on a variety of different substrates (Olson et al. 2012; Salehi Jouzani, Jouzani, and Taherzadeh 2015). However, cellulase-producing microorganisms are generally poorly characterized compared to model microorganisms such as *Escherichia coli* and *Saccharomyces cerevisiae*. Tools for genetic engineering of these microorganisms are also limited. Conversely, production of cellulase enzymes in more traditional industrial and model microorganisms has been achieved for a number of different systems (Kuhad et al. 2016; Percival Zhang, Himmel, and Mielenz 2006). However, the efficiency of cellulase production, secretion and activity remains a major obstacle to this approach (den Haan et al. 2015; Lambertz et al. 2014). Additionally, the requirement for tremendous new efforts of engineering a single microorganism to produce a new chemical of interest has also made this approach difficult from a practical standpoint. For these reasons, CBP conversion of lignocellulosic biomass via a single microorganism has been shown for only a few chemicals to date. Recently, a number of CBP systems have been designed to combine more than one microorganism. In these approaches, two or more microorganisms are cultured together, typically dividing the tasks of hydrolysis and production between microbial specialists. These systems are more modular, allowing different chemicals to be produced without major genetic redesigns. Enzymatic hydrolysis and bioconversion rates may be higher in specialist microorganisms compared to a single microorganism engineered to do both and the rates of different conversion steps may be more easily matched in order to increase productivity of the overall process(Tsoi et al. 2018). Several groups have successfully designed synthetic consortia-based CBP strategies for producing ethanol (Brethauer and Studer 2014b; Goyal et al. 2011; S. Kim et al. 2013; Speers and Reguera 2012; Zuroff and Curtis 2012). A synthetic consortium CBP system has also been designed for the production of isobutanol from lignocellulosic biomass by pairing the cellulolytic fungus *Trichoderma reesei* with an engineered isobutanol-producing *E. coli* strain (Minty et al. 2013). Several challenges must be addressed when a new molecule is selected as the production target for consortia CBP, which are inherently more complex than single-microorganism CBP. First, appropriate media composition must be achievable to allow microbial hydrolysis and bioconversion. Second, other compatibility factors, such as temperature, aeration and culture conditions must be satisfied. Finally, the activity level of each microorganism should be monitored in order to optimize the overall CBP process. In this work, the production of fumaric acid and lactic acid from microcrystalline cellulose and alkaline pre-treated corn stover by synthetic fungal consortia is demonstrated. In addition, a novel assay is developed for monitoring the

fumaric acid producing potential of the production specialist in the co-culture. Our progress represents a significant step towards establishing a robust, versatile and modular platform technology for consortia-based CBP conversion of lignocellulosic biomass to a wide variety of biochemicals.

1.2.2 Control of microbial consortia composition

Some synthetic consortia can converge towards stable community compositions without the need for external culture control. Often, however, synthetic consortia are unstable and will quickly become dominated by one organism or become extinct (H. J. Kim et al. 2008). Furthermore, tuning of microbial composition is a key tool for optimizing performance of productive consortia (Agapakis, Boyle, and Silver 2012; Johns et al. 2016). Several strategies have been previously used to control synthetic consortia composition such as pH preference tuning, spatially defined communities and cross-feeding enforced stability (Minty et al. 2013; Brethauer and Studer 2014b; Kerner et al. 2012). These strategies were inspired by natural microbial consortia (Nadell, Drescher, and Foster 2016). Although these strategies are effective for modulating or stabilizing community composition, there remain pitfalls in the application of existing controls for efficient production. For example, controls such as pH may be effective at tuning composition, but suffer from at least one organism spending at least half of the culture duration at a suboptimal pH. Genetically encoded composition controls, such as cross-feeding of metabolites is an effective stabilizing strategy. However, these systems must go through multiple rounds of genetic modification in order to optimize production and secretion of cross-fed metabolites. These systems also require very well controlled culture conditions and cannot easily tolerate slight changes of feedstock without genetic redesigns. For this reason, we sought to design a community composition control mechanism that does not sacrifice optimal culture conditions and that can be dynamically changed for new feedstocks or changes in culturing strategy. To that end, we have developed selective nitrogen delivery to control consortia composition for optimal production of fumaric acid. To our knowledge, selective nitrogen delivery has not previously been used to control consortia composition. Selective nitrogen delivery has the potential to be a superior control mechanism because it could be used to continuously control consortia composition during culture periods and to tune over a wide range of consortia composition ratios. All organisms require nitrogen for growth. Therefore, selective nitrogen delivery could also be used to control a wide variety of synthetic consortia. Acetamide is a very poor nitrogen source for wild-type *T. reesei* and *R. delemar*. In this work, we replace the *T. reesei* urease gene with the *Aspergillus nidulans amdS* gene, allowing *T. reesei* to efficiently use the uncommon nitrogen source acetamide, while eliminating its ability to use the common nitrogen source urea.

Chapter 2 High-resolution mapping of position-dependent expression variation in bacteria

2.1 Approach and results for mapping position-dependent transcriptional variation in E. coli

Here, we employ Tn5 transposase to perform massively parallel integration of a standardized reporter construct into over 144,000 sites across the genome to create an empirical map of gene-independent transcriptional propensity across the bacterial genome (Figure 2.1). High-resolution transcriptional propensity comparisons with genomic features can reveal both strong and weak correlations with high statistical power. To test the effect of genome position on gene expression, and not native promoter strength, we designed a reporter construct with very strong bi-directional terminators and its own inducible promoter (Y.-J. Chen et al. 2013). Each reporter construct is tagged with a unique barcode identifier, which allows simultaneous tracking of gene expression from thousands of integrations. Using a modified transposon footprinting procedure, unique barcodes were paired with integration location, allowing transcribed barcodes to serve as a reporter for the overall abundance of RNA or DNA at each integration address. The TetO1 promoter, which is recognized by the σ70 factor (and drives expression of most genes during exponential growth), drives expression of mNeonGreen fluorescent protein (mNG) followed by a 15 base barcode on the 3' UTR of the RNA upon induction by anhydrotetracycline (aTc) (Clavel et al. 2016). Criteria for reporter design were: 1) relatively small size and 2) low expression level, in order to minimize the effect of the reporter on the local genome context (T. B. K. Le et al. 2013a; Kosuri et al. 2013a). The inclusion of a protein on our construct ensures that the transcribed RNA will be subject to typical post-transcriptional phenomena (*e.g.*, co-transcriptional translation and subsequent protection by ribosomes). In keeping with efforts to minimize reporter size, the selection marker is an FRT-flanked kanamycin resistance cassette, which was removed by Flp recombinase before the full-scale profiling procedure (Fig. 1.1A).

2.1.1 Results

Based on our footprinting results, 144,000 random integration reporter barcodes were paired to their genomic integration location on the *E. coli* genome. Higher densities of reporter integrations were

present around the origin of replication (Ori), as expected due to higher Ori -Terminus chromosome copy number during exponential phase growth at the time of transformation (Fig 2A). On average, one unique barcoded integration is present every 33bp, greatly exceeding the resolution of position-dependent expression variation achieved by any previous works. To obtain information of the amount of RNA transcript produced per unit DNA present in a growing library (which we henceforth refer to as the transcriptional propensity at that location), we extracted matched RNA and DNA samples from exponentially growing samples of the reporter library during induction with aTc. The resulting sequencing data provided RNA and DNA counts of only reporter barcodes, which were then mapped to the corresponding genomic locations using the transposon footprinting data described above. Autocorrelation analysis was used as a quantitative measure of correlation between raw transcriptional propensity as bp distance between insertion sites increase to determine whether reporters integrated into similar locations also exhibit similar expression (Fig. 2.1A, B). We demonstrate that neighboring integrations have a high similarity of raw transcriptional propensity, which generally decreases as bp distance increases. Therefore, reporter transcription is non-random and dependent on integration location (Fig 2.1A, B). The RNA per DNA barcode values were smoothed with a rolling median around 500 bp windows for all integration sites with a minimum of three reporter integrations within the surrounding window. The replicates were quantile normalized and averaged. The resulting >90 k transcriptional propensities were mapped onto the *E. coli* genome. Transcriptional propensity variation appears roughly waveform at the whole-genome scale (Fig. 2.1E). The roughly periodic waveform pattern is also reflected in the autocorrelation plot (Fig. 2.1A, B). Several sharp troughs are also apparent, independent of the overall waveform. Transcriptional propensities are not a result of gene dosage resulting from high Ori-Ter ratios during exponential phase growth or from differing representation of a library member because all transcriptional propensities are reported as RNA per DNA ratios.

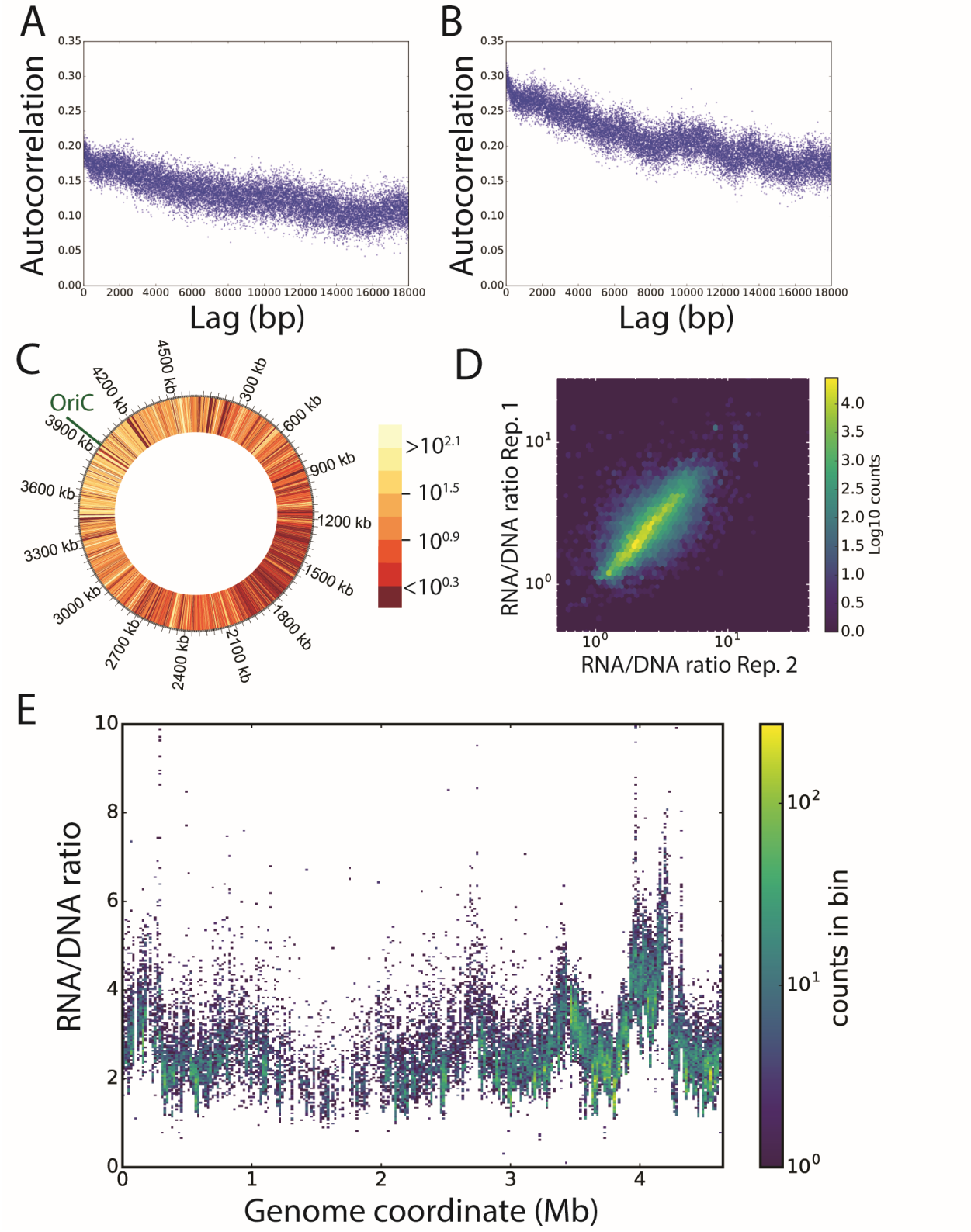
A
Autocorrelation
Lag (bp)
B
Autocorrelation
Lag (bp)
C
OriC
4500 kb
300 kb
4200 kb
600 kb
3900 kb
900 kb
3600 kb
1200 kb
3300 kb
1500 kb
3000 kb
1800 kb
2700 kb
2100 kb
2400 kb
>10^2.1
10^1.5
10^0.9
<10^0.3
D
RNA/DNA ratio Rep. 1
RNA/DNA ratio Rep. 2
Log10 counts
E
RNA/DNA ratio
Genome coordinate (Mb)
counts in bin

Figure 2.1: Genome-position dependent transcriptional propensity from random integration of a barcoded reporter is non-random. A) Autocorrelation of raw RNA/DNA ratio values for replicate 1. B) Autocorrelation of raw RNA/DNA ratio values for replicate 2. C) Reporter integration number for 1kb windows throughout the genome. D) Correlation between replicates for calculated transcriptional propensity from 500bp rolling median windows (Spearman ρ= 0.91). E) Transcriptional propensity (over 500 bp median rolling windows) mapped to specific integration locations on the *E. coli* genome. The color at each position indicates the number of unique transposon insertions contributing to the signal at that position.

Most strikingly, the seven ribosomal RNA operons in the *E. coli* genome are located within each of the major peaks of transcriptional propensity (Fig 2.2A).

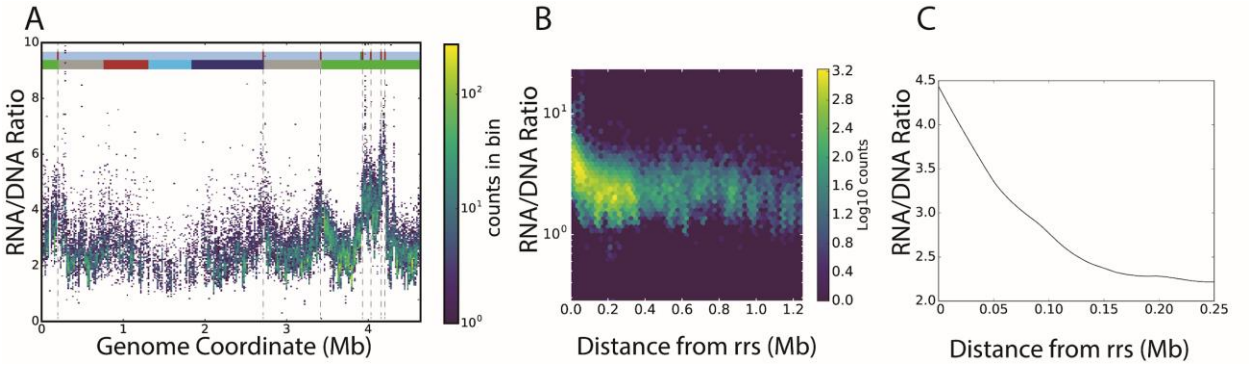

Figure 2.2: Transcriptional propensity peaks correspond to ribosomal RNA operon and macrodomain boundaries. A) Transcriptional propensity sinal (as in Fig. 2E) superimposed on other genomic features of interest. All seven ribosomal RNA operon locations are indicated in red on blue the upper bar. Macrodomains are indicated on the lower bar (Lioy et al. 2018a). B) Correlation of transcriptional propensity and distance from the nearest *rrs* operon (Spearman ρ= -0.56). C) Lowess fit of transcriptional propensity with rrn distance (Lowess Fraction = 0.33).

We next examined the correlation of transcriptional propensity with several characterized genomic features using rolling-window medians over 500 bp for each data set. Despite the fact that the abundant NAP Fis is not expected to bind the reporter construct, transcriptional propensity is highly positively correlated with Fis binding level at genomic integration sites (Fig 2.3A). Conversely, transcriptional propensity is strongly negatively correlated with H-NS binding (Fig. 2.3B)(Kahramanoglou et al. 2011b). These findings are consistent with a heterochromatin-like gene silencing role for H-NS. Protein occupancy is also negatively correlated with transcriptional efficiency, consistent with reporter silencing observed by Bryant et al. when integrated within tsEPODs (Bryant et al. 2014; Vora, Hottes, and Tavazoie 2009).

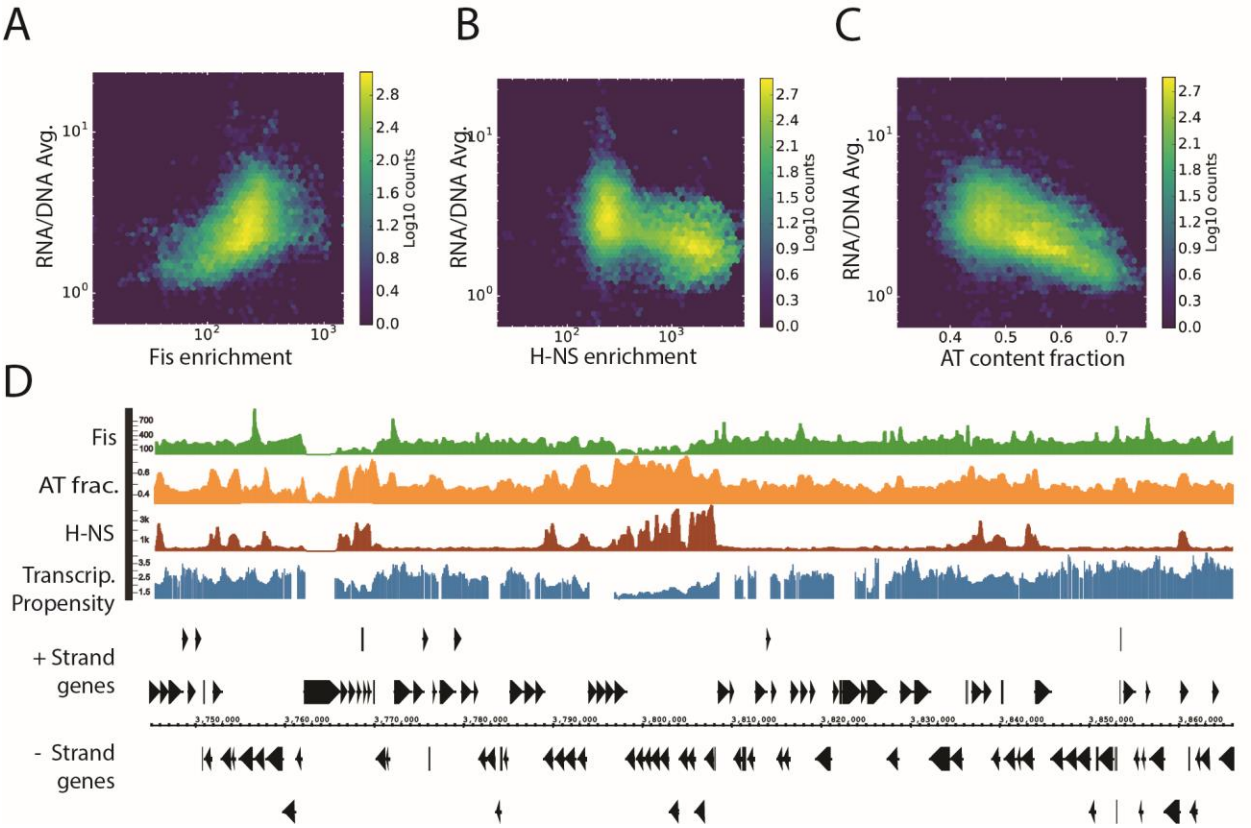

Figure 2.3: Correlation of transcriptional propensity with binding of abundant NAPs and nucleotide content. A) Correlation of transcriptional propensity with enrichment by Fis binding (500bp rolling median, Spearman ρ= 0.5) B). Correlation of transcriptional propensity with enrichment by H-NS binding (500bp rolling median, Spearman ρ = -0.58). C) Correlation of transcriptional propensity with AT content (500bp rolling mean, Spearman ρ = -0.59). D) Genome view of an H-NS silenced region and surrounding genomic context. Tracks from top to bottom for Fis binding, H-NS binding, AT content and transcriptional propensity. Strand-specific gene annotations are indicated below the data tracks.

Surprisingly, RNA abundance from native genes displays only a weak positive correlation with transcriptional propensity (Fig. 2.4A). However, when larger rolling median windows are used for RNA abundance from native genes and transcriptional propensity positive correlation increases (Fig. 2.4B). These results indicate that the regulatory logic governing expression of individual genes is likely dominant over the underlying transcriptional propensity of a given region.

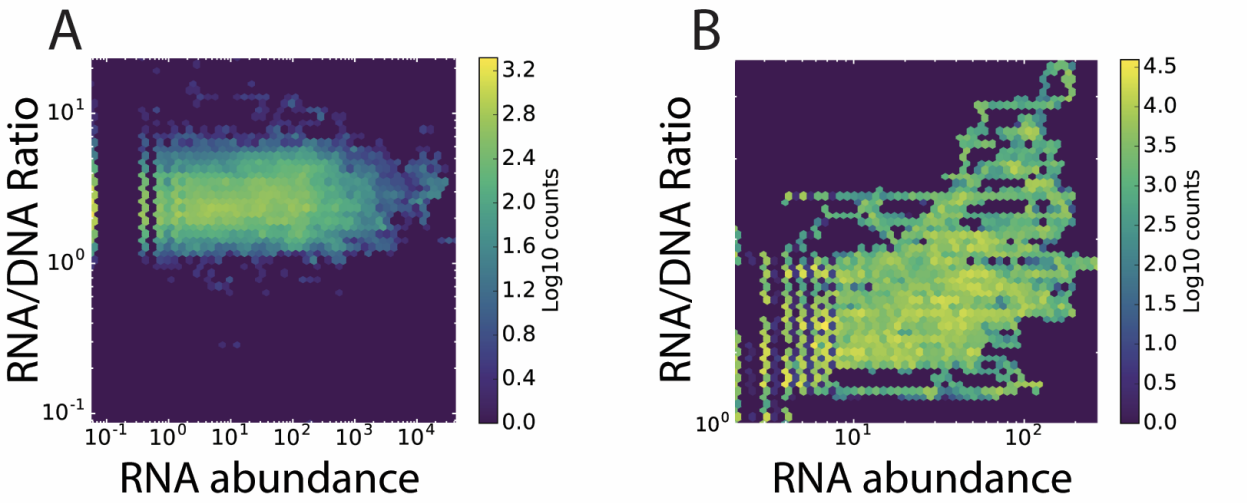

Figure 2.4: Correlation of transcriptional propensity with RNA abundance suggests native genes may be subject to regional variation in transcriptional propensity. A) Correlation of transcriptional propensity with E. coli native RNA abundance over 500bp rolling median window (Spearman ρ= 0.24). B) Correlation of transcriptional propensity with E. coli native RNA abundance over 50 kb rolling median window (Spearman ρ= 0.51).

We also examined the correlation of neighboring RNA abundance in all orientations relative to the reporter on transcriptional propensity (Fig. 2.5). Native RNA abundances resulting from tandem orientation (or co-directional) transcription with reporters have weak correlation with transcriptional propensity, similar to correlations with total RNA abundances (Fig 2.5B, D). These data indicate that even very high neighboring transcription may have only a mild impact on transcriptional propensity. Since native RNA abundances in the tandem orientation with respect to the reporter are very similar regardless of which is upstream, insulation by the strong upstream transcriptional terminator of the reporter is also validated. Transcriptional propensity in the divergent orientation with respect to the reporter integration is similar to the tandem orientations, with a mild decrease when RNA abundances are very high. There is a moderate decrease in transcriptional propensity when RNA abundances are very high from the convergent orientation (Fig 2.5D). Together, these results indicate that RNA abundance only mildly effects neighboring genes except for very highly expressed genes. These results are largely consistent with the careful mechanistic studies of orientation-dependent expression interference between genes on plasmids (Yeung et al. 2017). Transcriptional propensity from reporters on each strand display the same overall waveform pattern and are highly correlated (Fig. 2.5E). There is no evidence for a strand bias depending on the reporter direction with respect to replication.

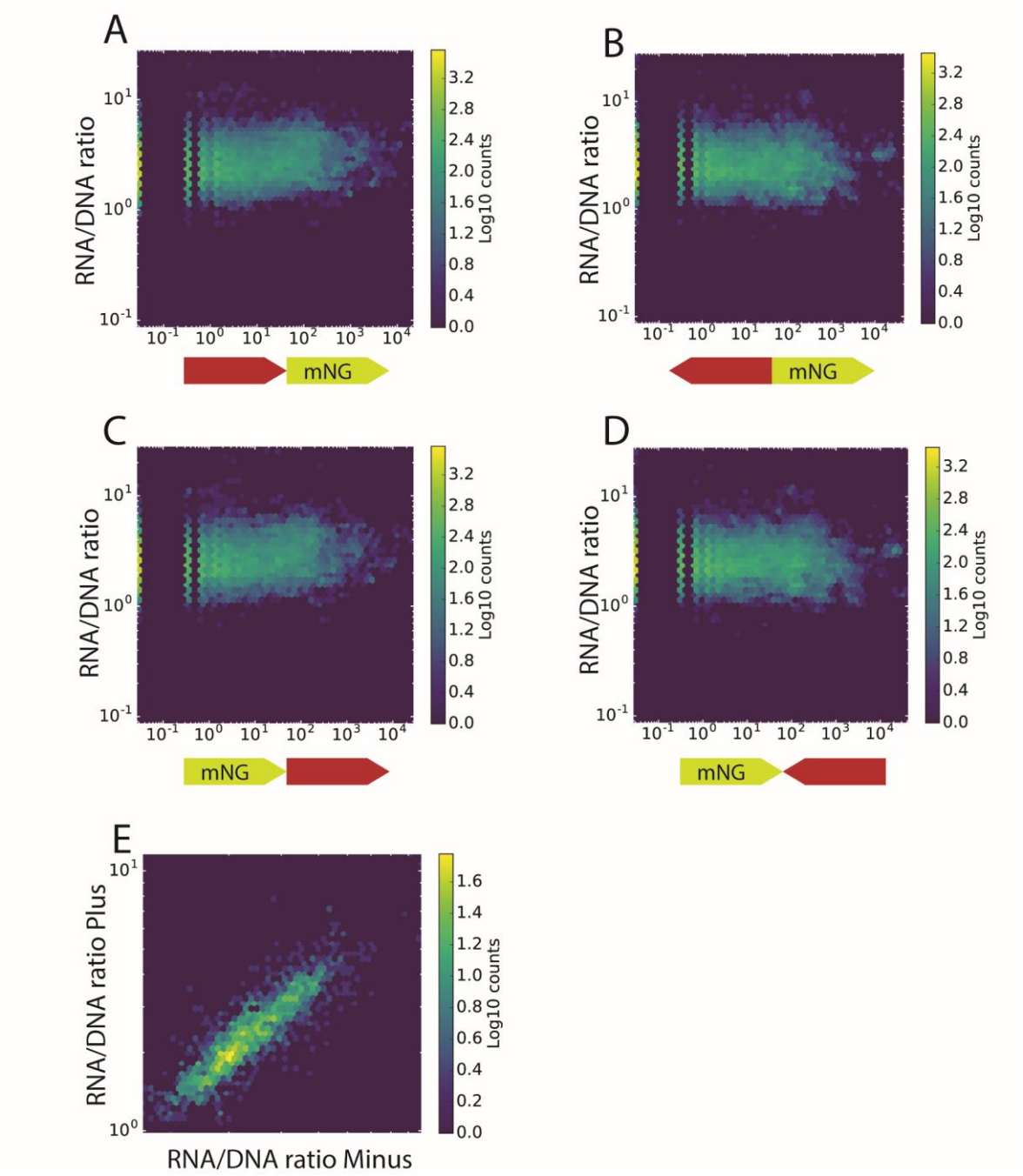

Figure 2.5 Effect of neighboring RNA abundance on directional transcriptional propensity and correlation of strand-specific transcriptional propensity. The cartoon shows the transcription direction of the reporter (mNG) on the + strand correlation with 500bp of native RNA abundance in the indicated transcriptional direction (red arrow). A) Tandem orientation considering RNA from 500 bp upstream of the reporter (Spearman ρ= 0.15). B) Divergent orientation (Spearman ρ= -0.05). C) Tandem orientation considering RNA from 500 bp downstream of the reporter Spearman ρ= 0.16). D) Convergent orientation Spearman ρ= -0.03). E) Correlation of transcriptional propensity on the plus strand with transcriptional propensity on the minus strand for shared integration locations (Spearman ρ= 0.9).

Other NAPs and DNA binding proteins were not well correlated with transcriptional propensity (Fig 2.6). We also found no correlation of transcriptional propensity with DNA supercoiling density.

Adenine and thiamine (AT) content in a 500 bp window around insertion locations was negatively correlated with transcriptional propensity (Fig. 2.3C). AT content is also highly correlated with H-NS and protein occupancy binding.

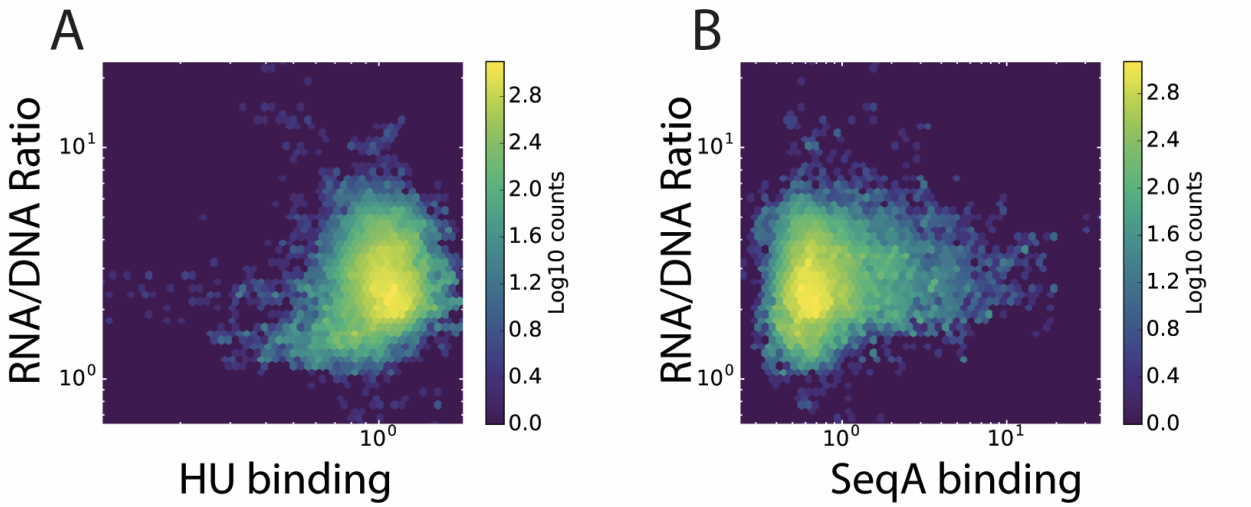

Figure 2.6: NAP HU and SeqA are poorly correlated with transcriptional propensity. A) Correlation of transcriptional propensity with HU binding (Spearman ρ= 0.13). B) Correlation of transcriptional propensity with SeqA binding (Spearman ρ= 0.14).

2.2 Materials and Methods

2.2.1 Reporter construct design

The mNG coding sequence was obtained through license from Allele Biotech (blank location). We put mNG under the TetR1 promoter and the B0030 ribosome binding site, which is predicted to have 30-fold lower translation initiation rate than the highest rate of a native gene in *E. coli. (Kosuri et al. 2013b; Espah Borujeni, Channarasappa, and Salis 2014)*. Upstream of the mNG cassette, an FRT-flanked kanamycin resistance cassette amplified from the Keio collection was introduced in the divergent orientation relative to mNG (Baba et al. 2006). Directly downstream of the mNG coding sequence, we introduced an Illumina i5 adapter primer complement sequence and an AscI recognition site for later barcoding of the integration construct. The reporter and antibiotic cassettes are flanked by the strong bidirectional terminators L3S2P21 and ECK120026481 (Y.-J. Chen et al. 2013). Finally the entire cassette is flanked by mosaic ends (MEs) to allow for binding to Tn5 transposase. The ME-flanked construct was modified to remove two PvuII restriction sites in order to allow for PvuII digestion of the plasmid pSAS31 and release the integration construct for Tn5 transposase binding *in vitro.*

2.2.2 Strain background design

MG1655 (CSGC 7740) was obtained from the Coli Genetic Stock Center (CGSC, Yale) (Blattner 1997). We used P1 vir transduction to introduce the Z1 cassette from MG1655 Z1 malE, a gift from Keith Tyo (Addgene plasmid # 65915) into MG1655. This MG1655 Z1 strain was then transformed with the lambda red plasmid pSIM5 (gift from Prof. Don Court). We then used the primers BT1promCh F and BT1promCh R to amplify the mCherry and ampicillin resistance cassette from pBT1-proD-mCherry, a gift from Michael Lynch (Addgene plasmid # 65823). The mCherry cassette was then integrated into a site directly downstream from *yihG* using lambda red recombination to produce ecSAS17 (MG1655 *malE*::Z1 *mCherry*$^{+}$ *AmpR*). We confirmed the mCherry integration by genotyping and the transduction of the Z1 cassette by observing TetR-mediated repression of mNG compared to a blank MG1655 strain. ecSAS17 was then transformed with the pBAD-Flp plasmid (see below) to provide the starting strain for library generation.

2.2.3 Large-scale plasmid barcoding

pSAS31 was digested with the restriction enzyme AscI. Primers were used to introduce the barcode and amplify the entire plasmid by PCR (Fig. 2.7). The resulting fragment was digested by DpnI and AscI, and then ligated with T4 ligase overnight at 14°C. The reaction was quenched with EDTA. We then scaled up the Hanahan procedure to transform chemically competent cells with the ligated plasmid (Hanahan, Jessee, and Bloom 1991). Cells were recovered in SOC for one hour at 37°C before removing an aliquot for transformation efficiency counts and adding kanamycin for 8h liquid selection at 37°C. Cells were then pelleted for 7 minutes at 4600 x *g* and snap frozen in liquid nitrogen. To obtain the plasmid, snap-frozen cells were resuspended in lysis buffer for plasmid miniprep.

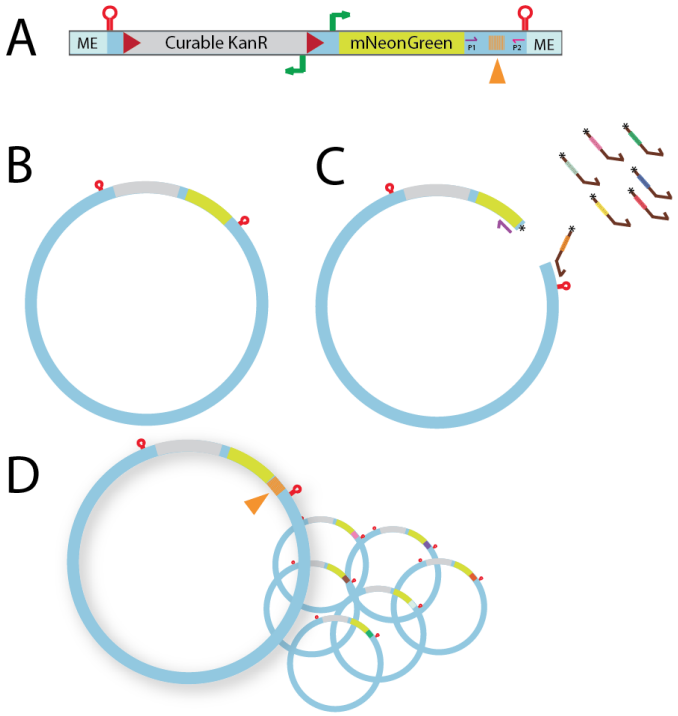

Figure 2.7: Barcoding of pSAS31 for generation of barcoded reporter integration construct. A) Diagram of the mature barcoded integration construct. The orange arrow indicates the position of the random barcode. B) Representation of key reporter features on the pSAS31 plasmid; the plasmid backbone (pale blue) is un-annotated for clarity. C) After digestion with AscI, pSAS31 is amplified with primers that introduce a random 15 bp barcode (brown primer). D) After digestion of the PCR product from (C) by AcsI, the plasmid is recircularized and transformed for selection. All plasmids in the library differ by only the barcode sequence. The orange arrow indicates the position of the random barcode.The barcoded integration construct is liberated by PvuII digestion of the plasmid library and used for transposome generation.

2.2.4 pBAD-FLP plasmid construction

The pCP20 plasmid causes over 90% of cells with an FRT-flanked kanamycin resistance cassette to lose resistance even at the uninduced 28°C temperature, presumably due to leaky expression of Flp recombinase (data not shown). Since Flp recombinase leaking from the pCP20 plasmid appeared to be severely reducing transposon integration efficiency, probably due the removal of the KanR cassette soon after integration and prior to liquid-phase selection, we replaced the PR temperature sensitive promoter on pCP20 with the arabinose-inducible promoter pBAD and repressor araC gene. The modified pBAD-FLP plasmid did not cause detectable loss of the KanR cassette under uninduced conditions (data not shown).

2.2.5 Tn5 integration of barcoded reporter constructs

To generate stable transposomes for electroporation into our target strain, barcoded pSAS31 plasmid was digested with PvuII for one hour at 37°C and fragments were separated on a 0.8% agarose

gel. The band corresponding to the integration fragment size was cut out of the gel and purified. 200 ng/µl fragment was then incubated with 2 µl Tn5 transposase and 1 µl glycerol according to the manufacturer's instructions. After 30 minutes incubation at room-temperature, the mixture was stored at -20°C. Electrocompetent cells were prepared using ecSAS17 with chloramphenicol included in the growth medium in order to maintain the pBAD-FLP Flp recombinase plasmid. 1 µl of the Tn5-DNA complex was mixed with 50 µl of fresh electrocompetent cells. Four separate electroporations were carried out at 1800kV and immediately resuspended in 1mL of 30°C SOC medium. Each reaction was pooled into SOC medium including chloramphenicol and incubated at 30°C for 1.5 hours. An aliquot for plating was removed from the recovery medium before adding Kanamycin. Liquid selection proceeded for 16 hrs at 30°C. After liquid selection, all cells were pelleted at 4600 x *g* for 7 minutes. Cells were then resuspended in 30 mL 15% glycerol, pipetted into 30 1 mL aliquots and snap frozen in a dry-ice ethanol bath before storage of the transposon library at -80°C (Girgis et al. 2007). According to colony forming unit counts from plating after recovery, 609,000 cells were uniquely transformed and maintained pBAD-Flp, as indicated by resistance to kanamycin and chloramphenicol.

2.2.6 Pairing integration site with barcode via transposon footprinting

Cells from one aliquot of the transposon library were recovered in 5 mL SOC for 30 minutes at 30°C with shaking. Genomic DNA was isolated from the library using the Qiagen Blood and Tissue kit for Gram negative bacteria. 1 µg of the resulting DNA was digested with either CviAII or CviQI restriction enzymes (each has a different 4 bp cut site but leaves compatible overhangs). An annealed Y-linker that complements the overhangs was ligated to the digested DNA fragments with T4 DNA ligase for 10 minutes. The reaction was quenched with EDTA. The DNA from the ligation mix was purified with Axygen AxyPrep Mag PCR cleanup beads at a 0.9:1 bead to DNA ratio to remove unligated Y-linker. The resulting DNA was amplified by PCR using the primers that bind within the transposon and on the Y-linker to amplify transposon-genomic DNA specific fragments. Illumina adapters were added to the resulting fragment by PCR.

2.2.7 Full-scale genome profiling procedure

The cryopreserved transposon library was scraped into 1 mL of M9-EZrich medium and diluted into 50 mL of M9-EZrich 1% Arabinose + 0.4% glycerol + chloramphenicol in a baffled 125mL flask to achieve OD of 0.0031 600nm. The flask was incubated at 30°C for 8 hours with shaking at 225 rpm to allow Flp recombinase to excise the kanamycin resistance cassette. Cells were then pelleted at 4600 x *g* for 7 minutes and resuspended in 50 mL PBS. In parallel, an aliquot of the culture was diluted and plated on LB-kanamycin and LB plates to determine the fraction cell that permanently lost kanamycin

resistance (<93%). Cells were pelleted again and resuspended in 10 mL M9RDM. Cells were then diluted into 100 mL of M9RDM + 100 ng/mL Anhydrotetracycline (aTc) to a final 0.0031 OD600. The culture was incubated at 37°C until an OD600 of 0.2 was reached (about 6 hours) to allow induction of the transposon-born reporter construct. The entire flask was then immediately transferred to an ice-slurry bath. Three aliquots of 5 mL were then pelleted at 6600 x *g* for 3 minutes and snap-frozen in a dry-ice ethanol bath to allow harvest of genomic DNA. In parallel, three additional aliquots of 5 mL of the culture was rapidly mixed with 25 mL Bacteria RNA protect reagent (Qiagen) and frozen according to the manufacturer's instructions to allow harvest of RNA from matched samples of the growing library. All samples were then stored at -80°C.

2.2.8 Nucleic acid processing and sequencing

Genomic DNA (gDNA) from harvested samples was extracted following the Qiagen Blood and Tissue kit instructions. 1 µg of gDNA was then digested for 1 hour with CviQI. The resulting DNA was purified with PCR cleanup kit and eluted into 0.1x TE. The DNA was then lightly amplified with primers flanking the barcode for eight cycles using Q5 polymerase, resulting in a 186 bp fragment. The DNA from the PCR mix was purified with Axygen AxyPrep Mag PCR cleanup beads at a 0.9:1 bead to DNA ratio to remove unincorporated primers.

RNA from the exponentially growing cells was extracted following the Qiagen RNeasy Bacterial RNA protect protocol including on-column DNaseI treatment. 1 µg of the resulting RNA and a single reverse primer were used for first strand synthesis with the NEB ProtoscriptII First Strand cDNA kit using the manufacturer's instructions, and the resulting cDNA was stored at -20°C. No-polymerase controls (-RT) were included. 20 µl of the cDNA or 5 µl of cDNA reaction mixture was used for a 50 µl minimal-cycle PCR amplification using NEB Q5 hotstart polymerase, following the manufacturer's instructions with the following modifications: NEB i5xx or i7xx primers were used to add Illumina adapter sequences. EvaGreen dsDNA dye to a final 1x concentration was added to each reaction. 10 µl of each reaction (including -RT controls) were then monitored for qPCR fluorescence signal during PCR amplification. The remaining 40 µl of each reaction was then amplified with the number of PCR cycles corresponding to 25% of the maximum fluorescence observed in the 10 µl qPCR pilot reaction. We verified that the cycle threshold for the -RT cDNA controls were at least 7 cycles greater than the standard cDNA samples (indicating background from DNA contamination of less than 1%). Each 40 µl PCR reaction was then purified with 90 µl of Axygen MAG-S1 beads and eluted in 0.1x TE. The purified DNA was was submitted the the University of Michigan sequencing core for sequencing on a NextSeq 550.

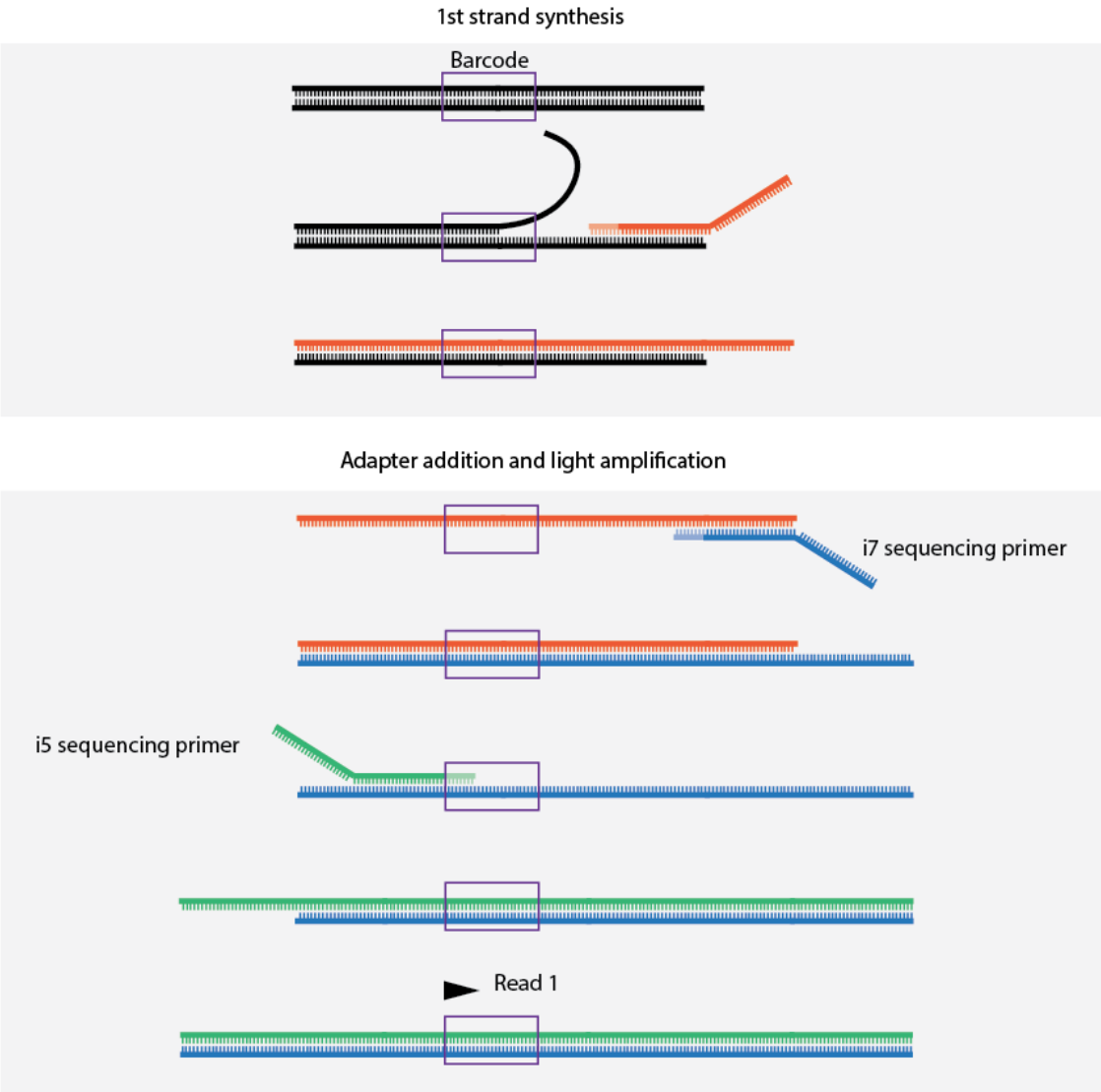

Figure 2.8: Nucleic acid processing for sequencing of RNA and DNA barcodes. The barcode (shown for DNA here) is indicated in the purple box. First strand synthesis introduces a UMI and a site for the i7 NEB sequencing primer to bind. Through a low number of cycles of PCR the library is lightly amplified for sequencing.

Chapter 3 Development of fungal consortia for consolidated bioprocessing of lignocellulosic biomass to organic acids

3.1 Development of production fungal consortia for fumaric acid production

The majority of section 3.1 has been previously published (Scholz et al. 2018).

The overall approach to consortia-based CBP is to divide the biochemical conversion steps between microbial specialists while satisfying the growth and production requirements of each member. By pairing the cellulolytic fungus *T. reesei* RaVC with the fumaric acid producing fungus *R. delemar* (NRRL 1526), one could theoretically convert lignocellulosic biomass to fumaric acid. Although these two filamentous fungi are not closely related phylogenetically, they were chosen as candidates for a CBP consortium because they share very similar growth condition requirements in liquid media.

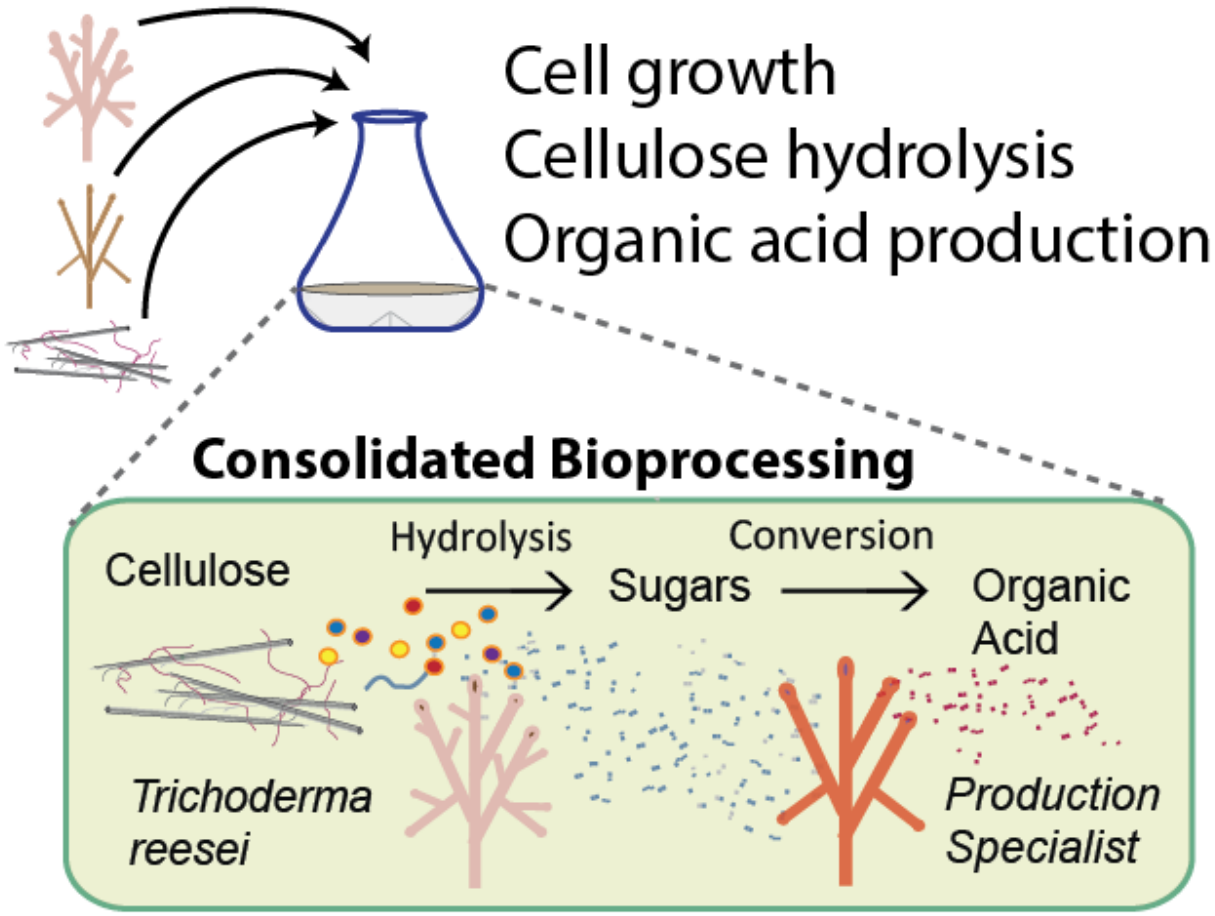

Figure 3.1: Overview of fungal consortia CBP conversion of lignocellulosic biomass to organic acids.

3.1.1 Fungal consortia design and baseline characterization of individual members

A defined minimal medium *Rhizopus-Trichoderma* co-culture medium (RTco) was formulated to allow both cellulose hydrolysis and fumaric acid production without the need for supplementation with expensive components such as yeast extract. *R. delemar* switches from growth to fumaric acid production phase when nitrogen is no longer available in culture media . Therefore, RTco was formulated with a nitrogen concentration that is 0.125 of those commonly used for *T. reesei* growth and cellulase production (Ding et al. 2011; Minty et al. 2013; Juhász et al. 2005). Under these conditions, both fungi are expected to grow until nitrogen becomes limiting in the production medium, at which point growth and cellulase production would cease, while fumaric acid production begins.

Each fungal strain selected above was first characterized in monocultures with the RTco medium. *T. reesei* monoculture grown on 40 g/L microcrystalline cellulose (MCC) in RTco medium efficiently accumulated glucose as expected under low nitrogen conditions (Fig. 1A). Under the proposed consortia CBP conditions 22g/L of glucose is produced from MCC at a productivity of 65

mg/L/h after 336 hours fermentation time (Fig. 1A). *T. reesei* monoculture was also grown on 20 g/L alkaline pre-treated corn stover (hereafter CS) in RTco medium. The CS utilized is composed of 47.8% and 21.2% of non-soluble glucan and xylan by weight, respectively. Glucan and xylan account for 95% of the carbohydrates in the CS. It was observed that 4.4 g/L glucose accumulated from hydrolysis of the CS, representing 41% of the theoretical maximum yield from glucan, while 0.86 g/L xylose accumulated, representing 15% of the theoretical maximum yield from xylan. Total sugar productivity was 22 mg/L/h over the course of 240 hours.

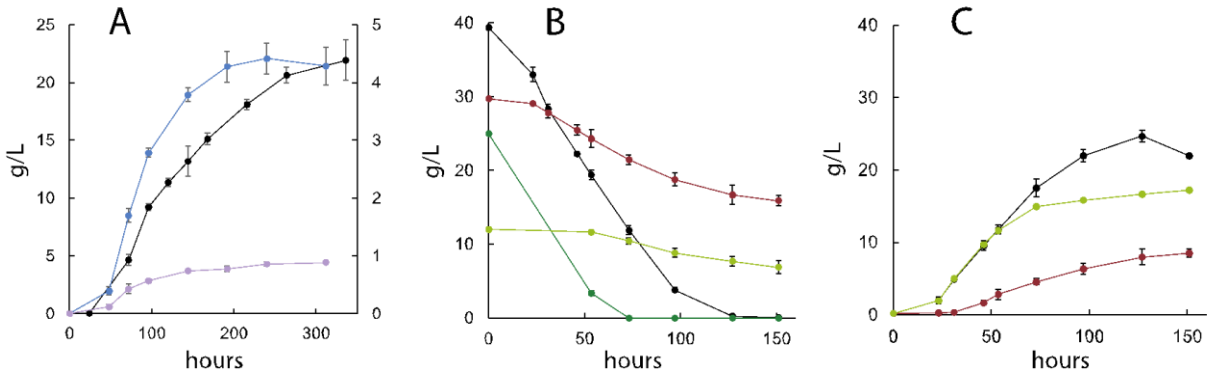

Figure 3.2: Monocultures exhibit efficient specialist activities in RTco medium formulated for co-culture. A) Sugar accumulation by *T. reesei* in two monoculture experiments: glucose (Black, left y-axis) from 40g/L MCC; glucose (Red, right y-axis) and xylose (Purple, right y-axis) from 20g/L alkaline pretreated corn stover. B) *R. delemar* monoculture can utilize pure glucose (Black), pure xylose (Red), or a mix of glucose (Dark green) and xylose (Light green) in RTco medium. C) *R. delemar* production of fumaric acid from sugar substrates corresponding to B). Data points in light green represent fumaric acid production from a mix of glucose and xylose.

R. delemar monoculture efficiently consumed 40 g/L glucose in RTco medium (Fig. 3.2B) to produce 22g/L fumaric acid (Fig. 3.2C), representing a yield of 0.55 w/w and a productivity of 153 mg/L/h. The theoretical maximum yield of fumaric acid is two moles per mole of glucose upon fixation of two moles of CO_2 in a reductive carboxylation pathway. By weight, 1.289 grams of fumaric acid would be produced per gram of glucose. However, this production pathway would not allow for production of ATP and requires CO_2 fixation (Roa Engel et al. 2008). Nitrogen concentration controls the tradeoff between cell growth and fumaric acid production (Ding et al. 2011). With minimal glucose substrate directed to cell growth, yields of up to 0.85 w/w from glucose have been reported (Kautola and Linko 1989). Consistent with previous observations with similar fungal strains , *R. delemar* was also capable of utilizing xylose as the sole or a portion of the carbon source in RTco medium to produce fumaric acid, albeit slower than on glucose. Recent efforts to select *Rhizopus* for growth and production on xylose as

the sole carbon substrate have achieved as high as 95% xylose utilization and 0.73 yield by weight (Liu et al. 2015), suggesting potential room for improvement compared to performance reported here. Additionally, *R. delemar* grown on medium containing mixed glucose and xylose demonstrated simultaneous usage of both sugars and accumulation of fumaric acid (Fig. 3.2B, C).

Results described above indicate the potential for *T. reesei* and *R. delemar* to be grown together for consolidated conversion of cellulose to fumaric acid in RTco medium. It should be noted that nitrogen concentration will be a crucial parameter in influencing the consortium's performance and there is a tradeoff between production yield and productivity.

3.1.2 Consolidated bioprocessing of cellulose into organic acids by synthetic fungal consortia

T. reesei and *R. delemar* adjustment cultures were simultaneously inoculated into RTco medium with 40g/L MCC as the sole carbon source at 1% of the total production culture volume each. A 600 mL culture in a 2.8L baffled flask was used to provide the large volume necessary to track multiple aspects of culture performance. Over duration of 316 hours, 88% of the initial MCC was degraded. Glucose concentration was observed to increase from an undetectable level to 18 g/L, which is 0.51 by weight of the MCC degraded over the fermentation duration or 0.45 by weight of total initial MCC (Fig. 3.3A). Fumaric acid was detected by HPLC analysis from an undetectable level at the time of inoculation to 3 g/L corresponding to a 0.08 w/w yield. Although MCC degradation was nearly complete, high glucose accumulation indicated that the conversion rate of glucose to fumaric acid was low compared to the rate of MCC degradation into glucose. The low glucose to fumaric acid conversion rate could be due to several factors. First, there may not be enough *R. delemar* cell accumulation. Second, the carbon and nitrogen ratio may not be appropriate for fumaric acid production, as *R. delemar* only produces fumaric acid once glucose becomes available and nitrogen becomes limiting. Finally, other factors in the co-culture such as secondary metabolites secreted by *T. reesei* could affect the physiology and hence the acid production capability of *R. delemar*. To dissect the state of the *R. delemar* cells, we developed an assay to measure the Acid Production Capacity (APC) of the *R. delemar* cells from the co-culture. In this assay, homogenous culture sample is removed from the production culture and washed with nitrogen-free RTco medium. The washed cells are then inoculated into nitrogen-free RTco medium with 20 g/L glucose as a substrate for conversion to fumaric acid. The APC is measured after a 24 hour conversion period with a unit of g/L/h (see more details in section 3.3.5). This quantity represents the maximum capacity for acid production of the *R. delemar* cells at a particular time point in the co-culture. We measured the APC at several time points during the co-culture. At 72 hours the APC was similar to the actual production rate averaged over the same time interval (Fig. 3.3B). The actual fumaric acid

production rate of the co-culture, however, dropped quickly afterwards and was essentially zero after about 200 hours. In contrast, the APC remained over 33 mg/L/h (Fig. 3.3B). This finding indicated that although the *R. delemar* mycelia remained capable of producing fumaric acid under the ideal condition, they were not producing fumaric acid at an appreciable level in the CBP co-culture, despite abundant glucose substrate. The co-culture medium may have become exhausted of one or more essential components for fumaric acid production, or inhibitory factors may have accumulated over time. Notably, the glucose production rate was relatively high compared to acid production rate throughout this experiment. These results highlight the need to develop strategies to match the rates of hydrolysis and production as an important direction for further optimization.

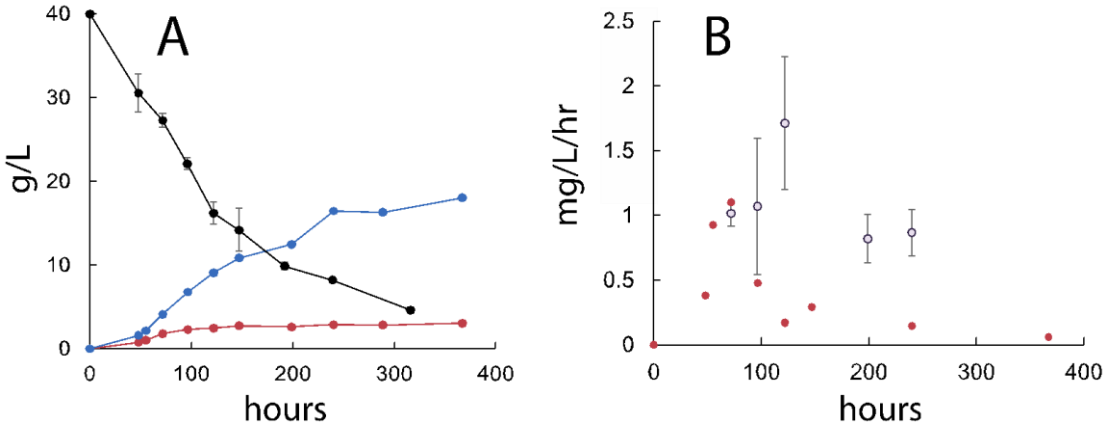

Figure 3.3: Fungal consortium produces fumaric acid from MCC. A) MCC degradation (Black, with error bars representing the standard deviation of two technical replicates in the gravimetric Updegraff assay), glucose accumulation (Blue) and fumaric acid production (Red) in a 600 mL bi-culture. B) The actual production rate in mg/L/h (Red), calculated for each time interval from the previous time point to the current one, was compared to the acid production capacity (APC) (Open circles, error bars representing the standard deviation of three technical replicates of the assay).

We also designed a lactic acid-producing consortium CBP system by replacing *R. delemar* with *R. oryzae* (NRRL 395) and carried out initial experiments using the same nitrogen concentration in TMM medium. Lactic acid titer of 4.4 g/L, representing a 0.11 w/w yield and 16.7 mg/L/h productivity, was achieved (Fig. 3.4). Due to observations that lactic acid may be degraded by *T. reesei* (Data not shown), we did not pursue further characterization of this consortium in the present study.

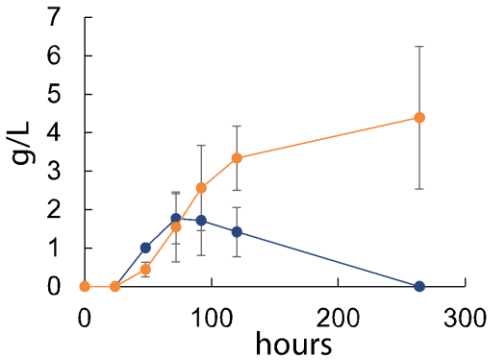

Figure 3.4: Lactic acid production from 40 g/L MCC using a modified fungal consortium. Glucose accumulation (Blue) and lactic acid accumulation (Orange) are indicated. Error bars represent the standard deviation from two replicates.

3.1.3 Effect of nitrogen concentration on consortium fumaric acid production

The tradeoff between fumaric acid production rate and yield from glucose by *R. delemar* can be controlled by nitrogen concentration (Liu et al. 2015; Ding et al. 2011). *R. delemar* monocultures with high nitrogen concentrations lead to more *R. delemar* cell growth and higher subsequent production rates of fumaric acid, but achieve lower final yields. In the more complex consortium CBP, the nitrogen concentration can still control the amount of carbon that is utilized for cell growth versus carbon directed towards producing fumaric acid. Therefore, nitrogen concentration should be a key parameter for optimizing the *T. reesei-R. delemar* consortium CBP system. To demonstrate the effect of nitrogen concentration on the production performance, we monitored consortium performance in RTco medium with three nitrogen concentrations. Nitrogen concentration variation led to different culture dynamics and production titer, yield and productivity (Fig. 3.5). Production medium with a low 5.88 mM nitrogen concentration allowed for relatively high amounts of glucose accumulation (Fig. 3.5A) and slow fumaric acid production, eventually achieving 0.148 yield by MCC weight and 16.6 mg/L/h productivity (Fig. 3.5B). Comparatively, an intermediate nitrogen concentration of 11.76 mM led to slow initial glucose accumulation and a decrease in glucose concentration at later time points, likely due to conversion into fumaric acid. Fumaric acid production under intermediate nitrogen concentration condition outperformed the other nitrogen concentrations tested in terms of yield (0.17 by weight), productivity (31.8 mg/L/h) and titer (6.87 g/L). In medium with the highest nitrogen concentration tested, 23.5 mM, almost no glucose accumulation was detected, fumaric acid accumulation was delayed, and the fumaric acid yield reached only 0.137 by weight. These results are consistent with a greater proportion of carbon being allocated for fungal growth under higher nitrogen conditions. However, the rate of fumaric acid accumulation under the high nitrogen condition did not exceed rates observed for intermediate

nitrogen concentrations, as we had predicted for higher cell densities. This apparent inconsistency is not surprising due to the low glucose accumulation, and is likely a result of glucose limitation due to allocation to cell growth. Promising future work for further engineering this consortium include optimizing the medium composition, particularly nitrogen concentration, that regulates the allocation of resources for cell growth vs. production, and developing new strategies to differentially regulate the growth of the two consortium members.

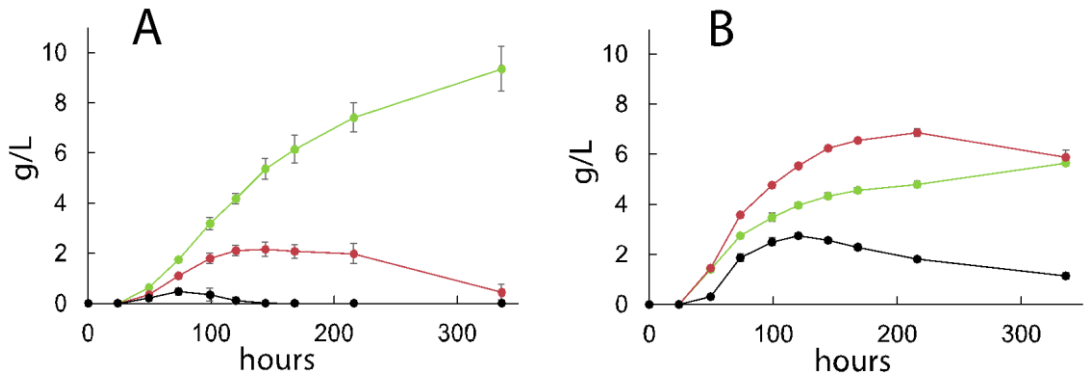

Figure 3.5: Nitrogen concentration is a key parameter for regulating consortium performance. A) Glucose accumulation under low (5.88 mM, Light Green), medium (11.76 mM, Red), and high (23.5 mM, Black) nitrogen conditions. B) Fumaric acid accumulation with nitrogen concentrations corresponding to A). Error bars represent the standard deviation from four replicates.

3.1.4 Consortium conversion of corn stover to fumaric acid

Lignocellulosic biomass is a complex substrate composed of crystalline cellulose, hemicellulose and lignin. In addition to these carbon compounds, nitrogen from proteins and other plant structures is present in all lignocellulosic biomass. For the present study, nitrogen concentration controls the flow of carbon between fungal growth and fumaric acid production. Therefore, the amount of nitrogen added to the culture medium must complement the usable nitrogen derived from the lignocellulosic biomass substrate. The fungal consortium was seeded into RTco medium containing 20 g/L of CS, which is composed of 9.6 g/L and 4.2 g/L of glucan and xylan respectively, under three different nitrogen concentration conditions. Similar to the performance on MCC, high nitrogen conditions led to fast substrate degradation and earlier cessation of fumaric acid production compared to lower nitrogen conditions (Fig. 3.6). The high nitrogen condition used for these experiments was 5.88 mM, one quarter of the high-nitrogen concentration used in the MCC experiments, but led to similar consortium dynamics. The differences in optimal nitrogen concentration between MCC and CS substrates are likely due to nitrogen derived from CS material. 0.69 g/L of fumaric acid was produced with a yield of 0.05 by weight from total initial fermentable carbohydrates. Overall consortium performance was considerably lower compared to those for MCC as the carbon substrate. As observed in numerous previous studies,

this reduction in performance is likely due to inhibitory compounds from the lignocellulosic biomass (Moreno et al. 2015; Ling et al. 2014). As in the MCC experiments, the fumaric acid production rate is far below the substrate degradation rate, indicated by the continuous accumulation of glucose (Fig. 3.6A). Although *R. delemar* is a promising consortium candidate because it efficiently converts sugars into fumaric acid and satisfies our major fungal consortia requirements, its acid production performance was low on corn stover substrates. *R. delemar* is found commonly as a fruit mold and is known to produce amylases and lipases which may aid in degrading natural substrates (Dolatabadi et al. 2014). However, *R. delemar* may not naturally encounter compounds found in the structural parts of plants. *T. reesei,* on the other hand, was relatively much more tolerant of the corn stover substrate, producing 0.46 w/w yield of glucose from total initial glucan solids and 0.21 w/w yield of xylose from total initial xylan solids in monoculture (Fig. 3.2A). Similar to approaches taken for yeast, selection of *Rhizopus* strains for lignocellulosic biomass tolerance may enable more efficient production (Almario, Reyes, and Kao 2013; Moreno et al. 2015; Pereira et al. 2014). Advances in xylose utilization or in tolerance to biomass toxicity may also help to improve consortium performance on real lignocellulosic biomass in the future.

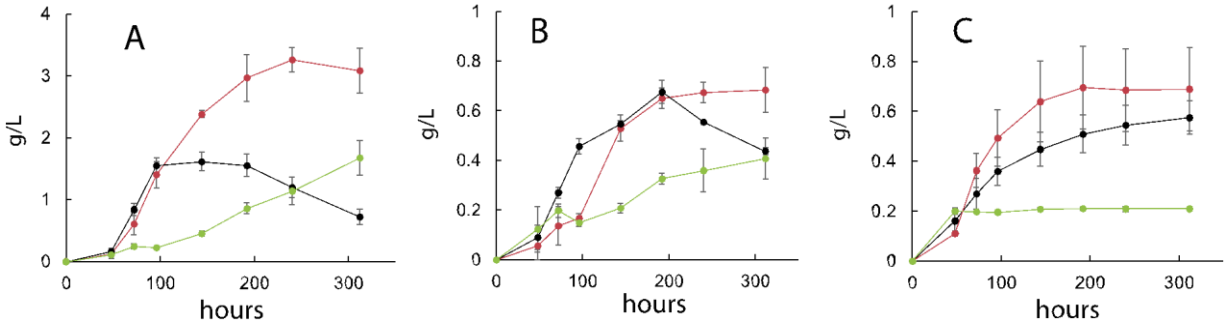

Figure 3.6: Fumaric acid production from alkaline pretreated corn stover by fungal consortium at different nitrogen concentrations. A) Glucose accumulation under zero (Light Green), low (2.9 mM, Red), and high (5.88 mM, Black) added nitrogen conditions. B) Xylose accumulation with nitrogen concentrations corresponding to A). C) Fumaric acid accumulation with nitrogen concentrations corresponding to A). Nitrogen added as a medium component is lower for all corn stover conditions in comparison to MCC experiments. Error bars represent the standard deviation of 4 replicates.

3.2 Engineering of Trichoderma reesei to control productivity of aerobic microbial consortia

The successful engineering of a fungal consortia capable of converting microcrystalline cellulose and lignocellulosic biomass into fumaric acid led us to ask whether the system could be further improved. Although final titer of fumaric acid is approaching the theoretical maximum, there is a substantial accumulation of glucose in MCC cultures for the majority of the fermentation period. This

indicates that the rate of MCC degradation into glucose is faster than the conversion of glucose into fumaric acid by *R. delemar*. This led us to speculate that increasing the relative abundance of *R. delemar* to *T. reesei,* and therefore their specialist activities, could improve overall productivity. In order to avoid common pitfalls in tuning community composition (discussion in section 1.2.2), we designed a strategy to selectively deliver nutrients to each consortia member. For this method, each organism has exclusive access to a limited nutrient to define the composition of the culture, and thus culture performance. To our knowledge, *T. reesei* and *R. delemar* have entirely overlapping nutrient requirements. For this reason, we sought to eliminate the ability of *T. reesei* to use urea as a nitrogen source while simultaneously bestowing it with the ability to use acetamide, which neither organism could previously use (Fig. 4.1). Nitrogen is an ideal nutrient to selectively deliver for CBP consortia for multiple reasons: 1) Nitrogen is one of the fundamental building blocks of life on earth and is required for all organisms to grow. 2) Nitrogen is present in low concentrations in many woody plants used as lignocellulosic feedstock. 3) The *Aspergillus nidulans* gene *amdS*, which codes for the enzyme acetamidase, is a common selection marker used for fungal transformations. Therefore, for theoretical and practical reasons, replacement of the *T. reesei* urease gene with the *A. nidulans* acetamidase gene was an ideal path to achieve selective nitrogen delivery (SND).

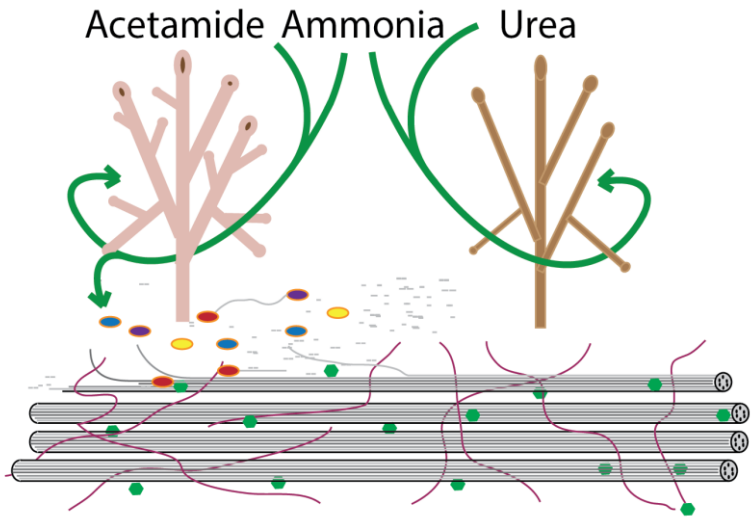

Figure 3.7: Theoretical nitrogen utilization capabilities under a SND strategy. Ammonia is available as a nitrogen source for both organisms. Acetamide is exclusively available by *T. reesei* (left). Urea is exclusively available to *R. delemar* (right). Arrows indicate the flow of nitrogen towards cell growth or cellulase production by *T. reesei* (colored ellipse).

Since acetamide and urea can freely diffuse into both cell types, it was essential that acetamidase or urease enzymes were not secreted to allow preferential access of each nitrogen source (Fig 3.8). We

note, however, that if the rate of acetamide or urea degradation greatly exceeds, the rate of ammonia uptake by either consortium member, ammonia may become usable by the other member by diffusion out of the cell (Eg. Acetamide converted to ammonia by *T. reesei* may be usable by *R. delemar*).

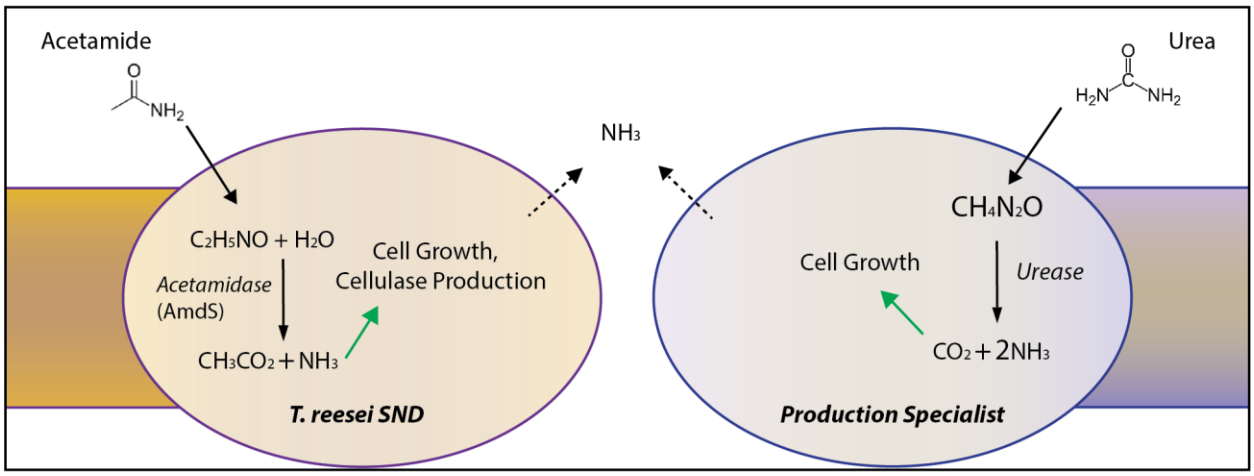

Figure 3.8:Conversion of the nitrogen sources acetamide and urea to ammonia. The dashed arrows indicate theoretical leakage of ammonia between consortium members.

3.2.1 Replacement of T. reesei urease gene with acetamidase gene.

The *A. nidulans* amdS gene, encoding acetamidase, has been used extensively to transform *T. reesei* and other filamentous fungi with episomes and by homologous recombination-based integration. We modified a previously developed the homologous recombination method to replace the *T. reesei* urease gene (https://genome.jgi.doe.gov/cgi-bin/dispGeneModel?db=Trire2&id=22705 protein ID 22705) with the amdS gene (Schuster et al. 2012). First, we cloned a 5.5kb fragment of of the urease gene and flanking region into pET24a+. Next, the plasmid was linearized by primers designed to retain the flanking homology regions of the urease gene (Figure 4.3a). The *amdS* gene derived amplified from the plasmid pBSamdS was cloned into the urease homology-pET24 backbone resulting in the pIG2 plasmid (Fig 4.3B). The mature integration construct was amplified from pIG2 by PCR (Fig 4.3C). Finally, 6ug of the integration construct was transformed into freshly harvested *T. reesei* Rut-C30 spores (US8450098B2) (Fig 4.3D).

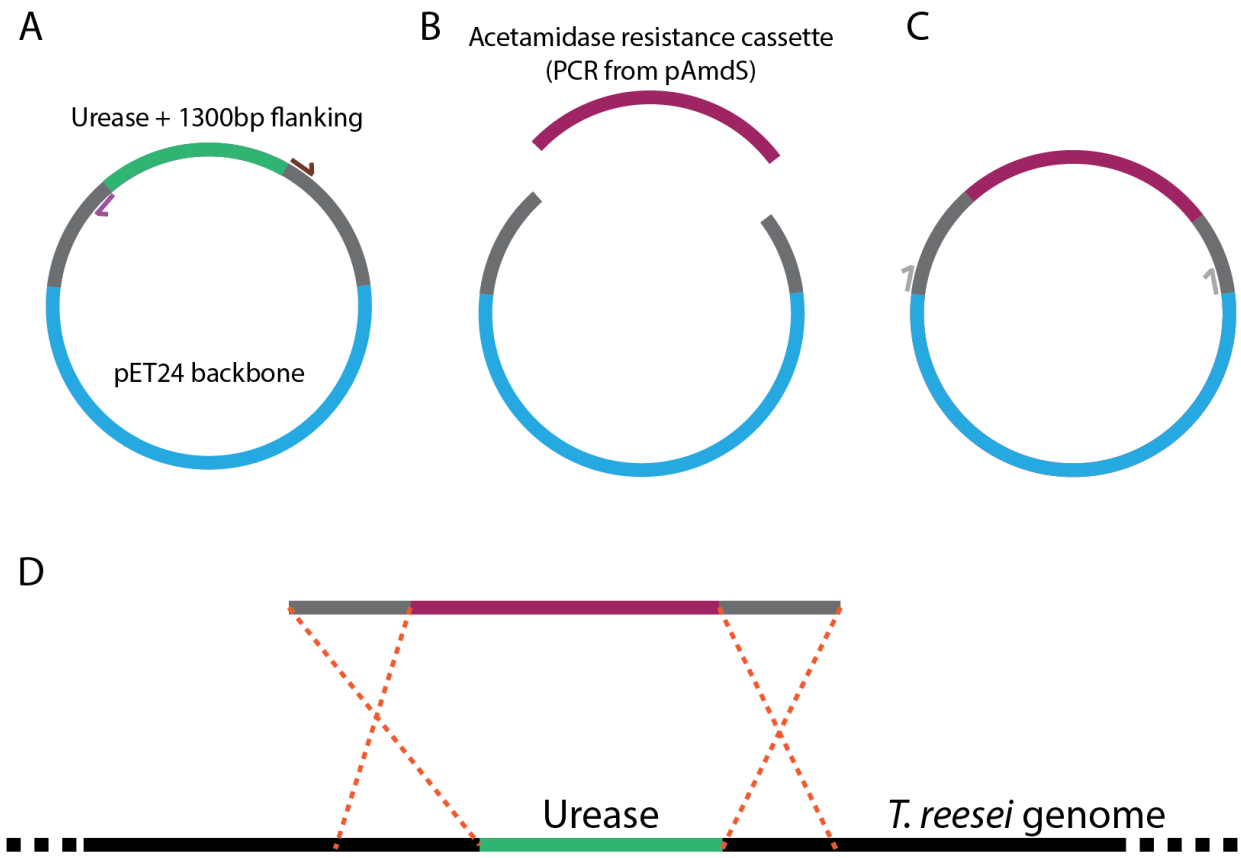

Figure 3.9: Cloning and transformation for replacement of the *T. reesei* urease gene with amdS. A) 5.5kb track of urease (green) and flanking region (grey) in pET24a+ backbone. B) replacement of urease gene with *amdS* to generate pIG2. C) PCR to amplify the mature integration construct from pIG2. D) Diagram of homologous recombination to replace the urease gene with amdS.

Transformants were isolated on selective medium. *amdS*+ colonies were streaked out twice on selective medium. Transformants with *amdS* replacing the urease gene were confirmed by PCR and termed *T. reesei* selective nitrogen delivery (SND).

3.2.2 Nitrogen utilization capability of SND

We next tested the nitrogen utilization capability of the SND strain. SND and the its parental strain Rut-C30 were grown in RTco with 10 g/L glucose as the sole carbon source. Each strain was grown on the same concentration of nitrogen in the form of urea, acetamide or ammonia as the sole nitrogen source. As previously reported, Rut-C30 grew well in urea and was capable of only minimal growth in acetamide. SND was capable of only minimal growth in urea and grew well in acetamide, confirming the new nitrogen utilization capability of SND (Figure 3.10). Both strains grew faster and reached a higher

dry cell weight (DCW) on ammonia compared to the other nitrogen sources. SND also reached a higher final density on ammonia compared to Rut-C30 for unknown reasons.

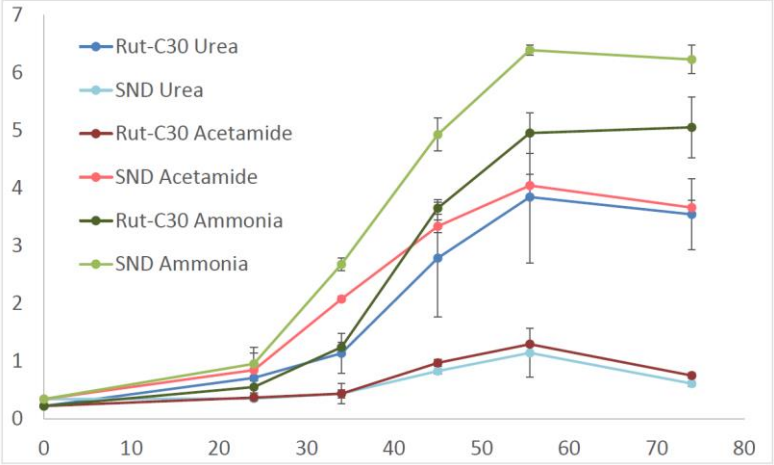

Figure 3.10: Nitrogen utilization capabilities of Rut-C30 and SND on various nitrogen sources. Rut-C30 or SND were grown on glucose as the sole carbon source. The nitrogen source was added in the form of urea, acetamide, or ammonia to the same final nitrogen concentration.

3.2.3 Selective nitrogen delivery to tune fungal consortium performance.

Under the same consortia conditions described in Chapter 3, SND and *R. delemar* (NRRL 1526) were grown in co-culture using MCC as the sole carbon source. The total nitrogen concentration was the same for all cultures in the form of ammonia or varying ratios of urea:acetamide. In terms of fumaric acid productivity and yield, 3:1 acetamide:urea ratio performed the best (Fig 3.11), and exceeded production of cultures without selective nitrogen delivery (Fig. 3.5). Very low concentrations glucose and fumaric acid were detected in urea only cultures, consistent with a nearly complete restriction of nitrogen from SND. As the proportion of nitrogen as acetamide increases, greater concentrations of glucose accumulate (Fig 3.11A). Between 1:1 acetamide:uea concentration cultures to acetamide only cultures, fumaric acid accumulation was roughly the same. These results demonstrate that reassignment of nitrogen utilization capability enabled selective nitrogen delivery for tuning of consortium performance for the CBP production of fumaric acid.

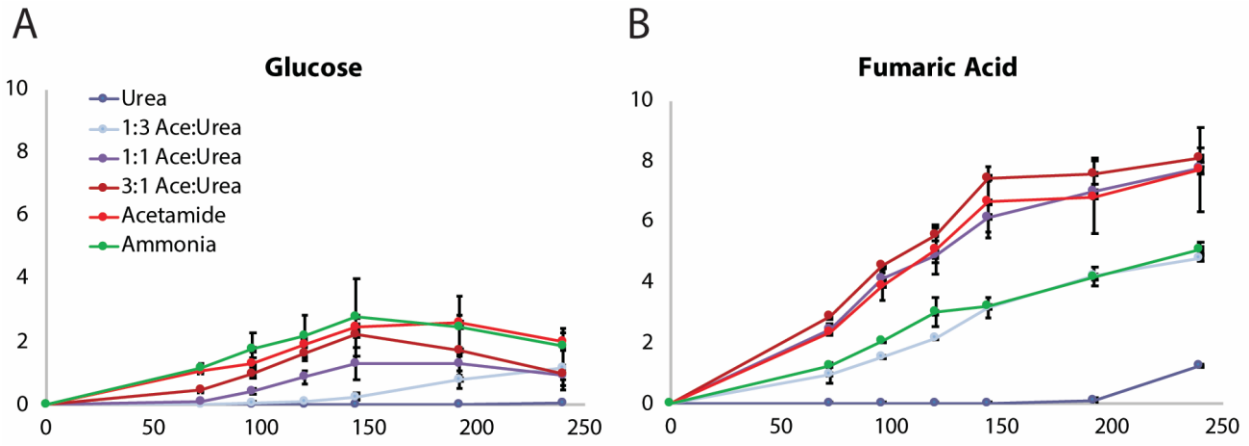

Figure 3.11: Acetamide:urea nitrogen ratio can tune fumaric acid production consortium performance. A) Glucose accumulation from co-cultures containing various nitrogen sources and ratios. Total nitrogen concentration is the same for all conditions. B) Fumaric acid accumulation from cultures corresponding to A.

3.3 Materials and Methods

3.3.1 Fungal strains and lignocellulosic biomass

Trichoderma reesei strain RaVC was generously provided by Mari Valkonen of the VTT Technical Institute (Finland). Rut-C30 was engineered to carry the RaVC fluorescent protein to yield the RaVC Rut-C30 *T. reesei* strain (Valkonen, Penttilä, and Benčina 2014). *Rhizopus delemar* (NRRL 1526) and *Rhizopus oryzae* (NRRL 395) were provided by the ARS culture collection (United States Department of Agriculture). Alkaline pre-treated corn stover was provided by the National Renewable Energy Laboratory (Golden, CO) with the following composition of non-soluble solids: ash 7.3%, ligin 17.8%, glucan 47.8%, xylan 21.2%, galactan 1.1%, arabinan 2.5%, acetate 0.1%).

3.3.2 Preservation of fungal strains

T. reesei spores were generated on potato dextrose agar (PDA) at 30°C. After 10 days, spores were washed with spore harvesting solution (9 g/L NaCl, 1 g/L Tween-80). Sterile glycerol was added to generate 20% glycerol spore stocks, which were stored at -80°C indefinitely. Cryopreserved *T. reesei* spores were directly inoculated into pre-cultures. *R. delemar* and *R. oryzae* spores were generated on potato dextrose agar (PDA) at 30°C after 7 days. Similarly, sterile glycerol was added to generate 20% glycerol spore stocks, which were stored at -80°C indefinitely. For all related experiments, cryogenically preserved spores were seeded onto PDA slants and grown for seven days before storage at 4°C. Spores from stored PDA slants were used within 3 months.

3.3.3 Culture media and conditions

Production cultures were grown in *Rhizopus-Trichoderma* co-culture medium (RTco) (0.5 g/L $(NH_4)_2SO_4$, 0.125 g/L Urea, 0.6 g/L $CaCl_2$, 0.4g/L $MgSO_4x7H_2O$, 0.3 g/L KH_2PO_4, 44 mg/L $ZnSO_4x7H_2O$, 10 mg/L $FeSO_4x7H_2O$, 2 mg/L $CoCl_2x6H_2O$, 1.6 mg/L $MnSO_4x4H_2O$, 0.0186% Tween-80 (v/v)) unless otherwise noted. The above nitrogen concentrations correspond to a total of 11.76 mM. Sterile $MgSO_4$, $CaCl_2$ and $FeSO_4$ solutions were added immediately before culture seeding, yielding the appropriate final RTco medium concentrations, in order to prevent precipitation. Carbon substrate was glucose, xylose, MCC or CS as indicated for each experiment. *Trichoderma* Minimal Medium (TMM) with a modified 11.76 mM nitrogen concentration was used for lactic acid production (40 g/L MCC, 0.5 g/L $(NH_4)_2SO_4$, 0.125 g/L Urea, 0.6 g/L $CaCl_2$, 0.6 g/L $MgSO_4x7H_2O$, 0.6 g/L KH_2PO_4, 1.4 mg/L $ZnSO_4x7H_2O$, 5 mg/L $FeSO_4x7H_2O$, 2 mg/L $CoCl_2x6H_2O$, 1.6 mg/L $MnSO_4x4H_2O$, 0.0186% Tween-80 (v/v)) *T. reesei* spores from cryostock were inoculated into 10 mL potato dextrose broth (PDB) and grown for 2 days at 30°C with shaking in a 50 mL conical tube to generate a pre-culture. Mycelia from the pre-culture were pelleted at 4600xg for 6 minutes and washed once in nitrogen-free RTco medium. 250 µl of mycelia resuspended in 10 mL of nitrogen-free RT-co medium were inoculated into 25 mL RTco medium with 20 g/L microcrystalline cellulose (MCC) and grown for 2 days in a 125 mL baffled flask to generate an adjustment culture. The adjustment culture was used to seed production cultures at 1% of total volume. *R. delemar* or *R. oryzae* were seeded from PDA spore slants into 100mL RTco medium with 20 g/L glucose and grown for 16 hours in a 500 mL baffled flask with shaking to generate a pre-culture. Mycelia from the pre-culture were pelleted at 4600xg for 6 minutes. Half of the mycelia from the resulting pellet was inoculated into 100 mL fresh RTco medium with 3 g/L glucose and grown for 3.5 hours in a 500 mL baffled flask with shaking to generate an adjustment culture. The adjustment culture was used to seed production cultures at 1% of total volume. Production cultures were grown using 25mL RTco medium in 125mL baffled flasks. The carbon substrate was 40 g/L of MCC or 20 g/L alkaline pre-treated biomass unless otherwise noted. Sterilization of the media was achieved through autoclaving for 15 minutes at 121°C. All cultures were grown at 30°C with 225 rpm shaking.

3.3.4 Quantification of consortia performances

Glucose, fumaric acid and lactic acid concentrations were determined by HPLC (Agilent 1100 with RID-10A detector equipped with a Rezex™ ROA-Organic Acid H+ (8%) column). Cellulose concentration was determined by using a gravimetric variation of the Updegraff assay (Ahamed and Vermette 2008; Antonov et al. 2016). All reported yield and productivity values were calculated from the time point with the highest titer for the compound of interest.

3.3.5 Acid production capacity (APC) assay

37.5 mL of homogeneous production culture mixture was centrifuged at 4600xg for 6 minutes. The resulting pellet was washed twice through repeated resuspension in 50mL nitrogen-free RTco medium followed by centrifugation at 4600xg. The resulting washed fungal mycelia and other solids from the production culture were then resuspended in 75 mL nitrogen-free RTco medium containing 20 g/L glucose and divided equally into three 125 mL baffled flasks. After a 24-hour culture period, fumaric acid accumulation was quantified using HPLC. Since the mycelia was diluted two fold during this process compared to the production culture, the fumaric acid concentration value was doubled to yield the reported APC value.

3.3.6 Alkaline pretreated corn stover preparation

Alkaline pretreated corn stover was obtained by kind donation from the National Renewable Energy Laboratory (Golden, Colorado). Slurry of the material was weighed onto a Whatman #1 wafer and subjected to vacuum. 1.6 mL Deionized water per gram of slurry was applied to the biomass and immediately washed through the Whatman paper by vacuum filtration. The resulting biomass was dried for 48 hours under vacuum. This biomass was weighed and included as described for each experiment.

3.3.7 Construction of T. reesei urease gene knockout cassette.

The urease gene and flanking region were amplified from Rut-C30 genomic DNA using primers for gibson assembly cloning of the fragment into the medium copy-number plasmid pET24a+ to generate pIG1. The amdS selection cassette was then amplified from pBSamdS, which was kindly provided by Dr. Monika Schmoll from the Austrian Institute of Technology (Vienna). The amdS cassette was then cloned into the pIG1 backbone generated by PCR to exclude the urease gene. The resulting plasmid, pIG2, was verified by sanger sequencing. The mature urease knockout cassette was amplified from pIG2 by PCR (Primer sequences: AAACGGGTTCATAGGGCGTA, CGGCAGCATTGAGAACATGA) and purified.

3.3.8 transformation and selection of the SND strain.

Rut-C30 spores from cyrostock were inoculated onto potato dextrose agar in 500 mL culture flasks at 30°C for 16 days. The resulting spores were collected with 10 mL of DI water. The transformation protocol was adapted from US patent 0304468. Briefly, spores were centrifuged at 3000 x g for 10 minutes and resuspended in 50 mL of ice-cold DI water. Another wash was conducted in ice-cold 1.1 M sorbitol. The resulting spores were resuspended in 500 mL of ice-cold 1.1M sorbitol. 100 ul of spores were then moved into an ice-cold 2 mm electroporation cuvette and incubated on ice with 6 ug of purified urease knockout cassette for 10 minutes. The spores were subjected to a pulse of voltage

2500. The spores were immediately resuspended in 1 mL of a 5:1 mixture of 1.1 M sorbitol and YEPD pre-warmed to 30°C. The spore suspension was then incubated for 16 hours at 30°C at 225 rpm. The spore mixture was then plated at multiple different concentrations on pre-warmed RTco minimal agarose medium selection plates containing 148 mg/L acetamide as the sole nitrogen source, 1 0g/L agarose, and 1.68 g/L cesium chloride. RTco was made as previously indicated. Filter sterilized cesium chloride and acetamide were added after autoclaving to avoid degradation of acetamide or heat-induced reactions from occuring. Colonies appeared approximately 48 hours after plating, with additional colonies appearing as late as 96 hours after plating. Individual colonies were cut out of the selection plates with a sterile spatula and placed on a fresh selection plate. After 48 hours, sections of mycelia far from the original seeding of the secondary plate were cut out and split divided for plating on selection plates or plates with urea as the sole nitrogen source. Using this method, we identified two colonies that grew robustly on acetamide plates that only grew minimally on urea plates. These strains were grown up on RTco selection plates with MCC as the sole carbon source for 24 days. The resulting spores were harvested with spore harvesting solution and stored in 20% glycerol at -80°C indefinitely. Note that this method requires selection plates to be monitored regularly, as mycelia from isolated colonies rapidly grow over each other. Additional platings on selective medium are recommended if any ambiguity in the genotype or phenotype of the transformed strain is observed.

Chapter 4 Conclusions and future perspectives

4.1 Discussion on transcriptional propensity findings in context of previous findings

Random integration of barcoded reporters in *E. coli* allowed mapping of transcriptional propensity at high density across the genome. Previously, a barcoded reporter has been integrated into 27,000 sites in mouse embryonic stem cells using piggyBac transposition, revealing a stronger association of low transcription with lamina-associated domains than H3K9me2 histone modification (Akhtar et al. 2013). To our knowledge as many as 38 sites have previously been tested in a single study for position-depending expression variation in bacteria (Jeong et al. 2018). Here, we used Tn5 random transposition to integrate into 144,000 unique sites into the 4.6 Mb *E. coli* genome, to produce the most high-resolution gene-independent expression mapping to date. This resolution uniquely allowed testing of reporter transcription from multiple sites within genomic neighborhoods with rare and distinct features. In addition, transcriptional propensity could be tested for correlation with known genomic features with high statistical power.

4.1.1 Transcriptional propensity and ribosomal RNA operons

Large peaks of transcriptional propensity across the genome are centered on ribosomal RNA operons (*rrn*) (Fig. 2.3A). *rrn* are the most highly transcribed genes in the *E. coli* genome, with an RNA polymerase every 85 bp compared to every 10-20 kb for the rest of the genome (French and Miller 1989) and reviewed in (Paul et al. 2004). In addition, plasmid encoded *rrn* physically relocate RNAP away from the nucleoid, which also causes a decrease in growth rate (Cabrera and Jin 2006). With the exception of *rrnC*, *rrn* also physically colocalize (Gaal et al. 2016a). Regardless, we find that *rrnC* is also within a transcriptional propensity peak. Together, these findings suggest a model in which very high concentrations of RNAP involved in active transcription of *rrn*, also increases transcriptional propensity of the local region. Bacterial species frequently have multiple *rrn* ranging up to 15 copies (Rainey et al. 1996). *rrn* Copy number correlates with rate of colony formation upon exposure to nutrients (Klappenbach, Dunbar, and Schmidt 2000).

4.1.2 Transcriptional propensity and NAP binding

Transcriptional propensity is highly correlated with binding of the epitope tagged NAP Fis, identified from chIP-seq experiments (Kahramanoglou et al. 2011b) (Fig. 2.4A). Interestingly, Fis also activates transcription from rrn promoters P1 through association with RNAP, but is not required for normal *rrn* regulation (Bokal, Ross, and Gourse 1995; Ross et al. 1990). Binding sites for Fis, identified through *in vitro* binding assays, are between 71 bp and 181 bp upstream of *rnn* transcription start sites (tss) (Hirvonen et al. 2001). In comparison, the reporter used in this study is relatively small, with the tss 157 bp from the edge of the integration construct. Therefore, it is possible that Fis activates reporter transcription through binding to local regions around integration sites in a similar manner to *rrn* transcriptional activation.

We observed a strong negative correlation of transcriptional propensity with the epitope tagged NAP H-NS from chIP-seq experiments, consistent with a silencing role (Kahramanoglou et al. 2011b) (Fig 2.4B). H-NS binds to AT-rich regions and can oligomerize along DNA using non-specific electrostatic interactions with DNA (Gao et al. 2017b). This phenomenon may explain why H-NS binding is highly correlated with transcriptional propensity, despite the fact that the reporter is not expected to bind H-NS on its own. We also find that integration density is most highly correlated to H-NS binding and with genomic AT content. Although this is only an observation for the present study, it suggests a model in which foreign DNA may more readily integrate into H-NS-bound and high-AT content sites and thereby increase the likelihood that they are silenced, as has been previously suggested (Fang and Rimsky 2008; Higashi et al. 2016). Horizontally acquired genes have a relatively high AT content compared to the *E. coli* genome average. Despite having a 53.7% GC content, the integration construct was still silenced in H-NS-bound regions. We also observed very low expression from reporters integrated into tsEPODs, strongly supporting and expanding on previous functional tests from a small number of sites (Bryant et al. 2014; Vora, Hottes, and Tavazoie 2009). Note, however, that these sites were not silenced to the extent that integrations could not be selected for in kanamycin-containing media.

4.1.3 Transcriptional propensity and physical properties of the chromosome

We also examined the effect of native RNA abundance, which is well correlated with the rate of transcription (H. Chen et al. 2015), in an orientation-specific manner. For the tandem orientation, regardless of whether the RNA abundance under consideration was upstream or downstream of the reporter, was mildly positively correlated with transcriptional propensity. Conversely, transcriptional propensity decreases for integrations neighboring the most highly transcribed genes in the convergent, and to a lesser extent divergent, orientation, which is mostly consistent with previous findings at couple

sites (Bryant et al. 2014) and on a plasmid (Yeung et al. 2017). Perhaps the impact of transcriptional interference would be more pronounced for highly expressed reporters. The relatively moderate effect of even very high neighboring transcription on transcriptional propensity may also indicate efficient DNA supercoiling regulation on the chromosome.

4.1.4 Functional follow up on transcriptional propensity findings

The findings described above raise a number of questions about the biological mechanisms underlying transcriptional propensity in *E. coli.* The first question that we are planning to address is: What does transcriptional propensity look like for bacteria growing in different conditions? For example, would peaks centered around *rrn* be retained during stationary phase and how would their magnitudes change? Gaal et al. observe that rrn loci continue to colocalize during stationary phase, albeit to a lesser degree (Gaal et al. 2016b). On the other hand, *rrn* transcription ceases during stationary phase. In order to test this question, we are planning to perform all of the same steps described here for stationary phase. However, a different set of promoters are active during stationary phase, which poses the question: What is best reporter design for testing transcriptional propensity during stationary phase?

Related to this problem, we are testing how transcriptional propensity affects other genes. We are addressing this point using two different methods. The first is to test a subset of genomic loci with several reporter variants. Although relatively low throughput, these experiments can be used to reveal the interplay between reporter gene features and genome context. The second method is to test the functional impact of features, such as proximity to *rrn* on reporters and native genes. For example, by knocking out a subset of the seven *rrn*, we will assess both the expression of a neighboring reporter and the expression of native *E. coli* genes via transcriptome analysis. The outcome of this functional testing will have implications for the generalizability of transcriptional propensity and how we think about the evolution of gene expression and genome organization in bacteria.

We will also test the impact of Fis and H-NS knockouts on transcriptional propensity. To our knowledge, there have been no studies to report position-dependent expression variation of a standardized reporter in a mutant background. H-NS binding frequently overlaps with tsEPOD peaks in *E. coli*, which indicates that some proportion of tsEPODS is made up of H-NS. However it is unclear what role other NAPs play in tsEPODS or whether there is functional overlap with H-NS. For example, StpA, an H-NS paralog and binding partner, displays highly overlapping binding with H-NS, as determined by chIP-chip. In addition an *hns stpA* double mutant displays a more severe growth phenotype than either single mutant (Uyar et al. 2009b). These data hint that other factors, such as StpA, may have partial redundancy in H-NS function. Similarly, we are planning to test the functional effect of a *fis* knockout.

Although Fis and H-NS may have functional roles in affecting transcriptional propensity, knockout studies may not be sufficient to fully understand their roles due to potential functional redundancy. Therefore, we should also be prepared to expand our functional testing to other NAPs and to study interplay between NAPs and other factors that may control their binding specificity.

Since the inception of this project we have also wondered whether there are any position-dependent translation effects. At least one study has found that the general trend of RNA expression was the same as the fluorescence level of a GFP reporter (Block et al. 2012a). However, there was no follow up to determine whether an increase in RNA level also led to a stoichiometric increase in GFP. Regardless, these results are in line with the canonical view that the amount of protein translated is determined by the RNA amount and intrinsic RNA features, such as ribosome binding site strength and secondary structure. To our knowledge, there has never been a systematic study to test whether the position that an RNA is transcribed from affects translation initiation rate. Possibly, genome position may be one of the factors that explains the poor correlation between RNA and protein level in bacteria (Lu et al. 2007). We are currently evaluating ribosome profiling data collected from the library described in this work to test whether gene position affects the rate that a transcript is being actively translated. Briefly, we are using the ratio of ribosome-bound barcoded reporter transcripts to the total count of each barcoded transcript to create a map of position-dependent translation propensity.

4.1.5 Evolutionary perspective of position-dependent expression variation and of self-assembly of distinct cellular regions

To date, extensive evidence demonstrates that bacteria have self-assembling exclusive zones within the cell, despite not having membrane separated compartments. As a simple example, the nucleoid is so dense and compact that it physically excludes large subcellular machinery, such as polymerases and ribosomes (Jin and Cabrera 2006b). The nucleoid can further sub-compartmentalize into regions called chromosome interacting domains (CIDs) (Lioy et al. 2018a; T. B. K. Le et al. 2013b). We are particularly interested in whether nucleoid structure is functionally relevant for transcription. Beyond these interesting mechanistic questions, we can also start to ask how structures and transcriptional propensity evolved. For example, does genome organization evolve over time for highly expressed genes to relocate to *rrn* proximal regions, or do genes more quickly evolve to regulate their own expression despite the genomic context. The fact that transcriptional propensity poorly correlates with native RNA abundance using 500 bp windows, but is highly correlated using 50 kb windows suggests that both evolutionary paths likely occur (Fig. 2.5).

In order to better understand the evolution of bacterial genome organization, we would need to better understand the relationship of relative gene order, which is stable among related species, and bacterial and transcriptional-propensity (Rocha 2008). *Bacillus subtilis* and *Caulobacter crescentus* would be particularly interesting to perform the Tn5 random integration of barcoded reporters method because there are several works that have elucidated the nucleoid structure and, to some extent, the mechanism controlling structure (T. B. K. Le et al. 2013b; T. B. Le and Laub 2016; Marbouty et al. 2014).

In addition to understanding the evolution of genome structure, we are also interested in better understanding the evolution of tsEPOD formation. Although AT content is well correlated with H-NS and tsEPODs, there are likely other factors that either promote or inhibit tsEPOD formation.

4.1.6 Outlook on applications of findings and future work for genetic engineering

Although we do not yet fully understand the mechanisms underlying transcriptional propensity variation, we can use the empirical maps to modulate gene expression. In a simple example, we have identified the genomic regions with the highest transcriptional propensity, which, when transformed for the DNA dosage, may be useful for overexpression of genes for biotechnology applications (Fig. 4.1). Furthermore, since there is natural variation in transcriptional propensity, can we use our predictions to create synthetic regions or construct with unique or extreme expression? Many labs have made substantial modifications to genomes of various organisms for studies ranging from minimizing genomes, eliminating horizontally acquired regions or shuffling genetic material for selection of new phenotypes. However, the transcriptional propensity data presented here may allow for design of genomes or genomic regions beyond simple knockouts and non-specific rearrangements.

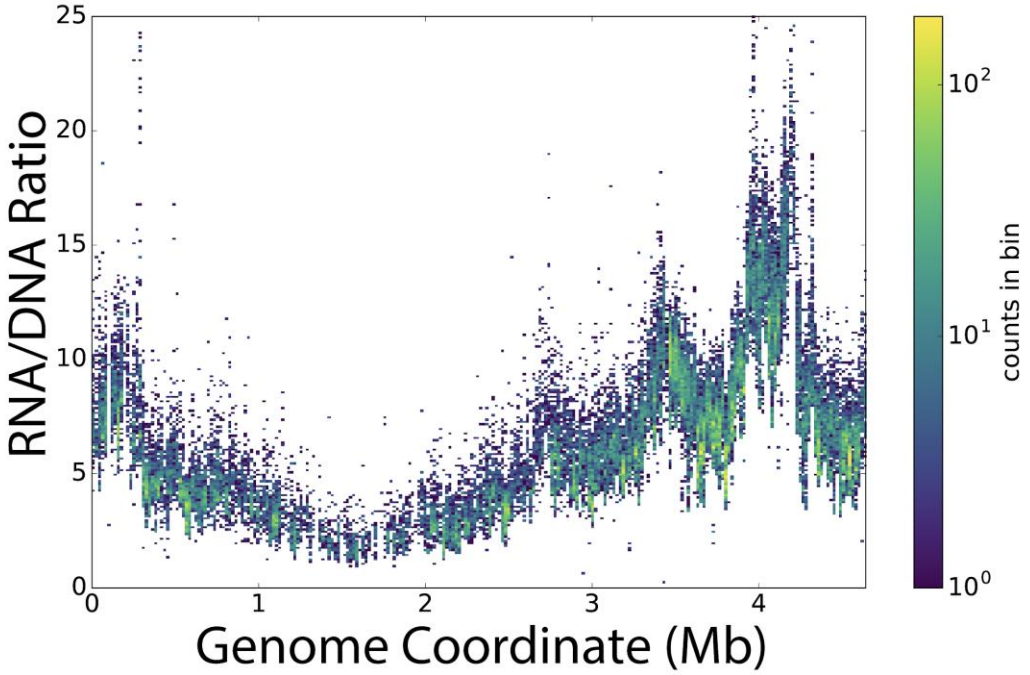

Figure 4.1: Dosage-scaled transcriptional propensity. Transcriptional propensity as in figure 2.2 transformed to reflect the DNA copy number for cells grown under the same conditions.

4.2 Perspective on fungal consortia results and on consortia CBP as an industrial platform

We demonstrated proof-of-concept of a synthetic consortium for CBP-based production of fumaric acid. Despite increasing attention from academics and some notable successes, there are still relatively few established productive systems that use more than one organism in a single reaction vessel (McNeil et al. 2013; Marmann et al. 2014). Our work highlights some of the the addressable technical challenges that may be limiting the field, which I will discuss generally and from the perspective of our research in the following sections.

4.2.1 Design of new consortia-based CBP systems

The goal of this work was specifically to convert lignocellulosic biomass into a commodity chemical. As discussed in introductory section 1.2, the major benefit to consortia-based CBP is specialization between consortia members and potentially decreased need for frequent genetic redesigns. Most specifically, specialization is desirable because engineered model organisms have been far less efficient and producing cellulase enzymes for degradation of lignocellulosic biomass (den Haan et al. 2015). Conversely, efficient cellulase producing organisms are currently difficult to genetically

engineer for production of commodity chemicals and the genetic engineering toolset is much more limited compared to model organisms. Therefore, both practical considerations and the potential benefits of species specialization motivated our work on consortia-based CBP. Since there are few studies use multiple co-cultured organisms as the basis of an engineered system, I will highlight, in roughly chronological order, some of the challenges with engineering a new system.

Assuming an appropriate target molecule is identified, there are multiple important considerations to take into account when designing a new consortia-based CBP system. Organisms involved must satisfy the following criteria: 1) Similar media requirements without the need for costly components (eg. yeast extract, peptone...etc). 2) Similar temperature, pH and aeration requirements. 3) Tolerance to the target molecule. 4) Species do not degrade the target molecule. 5) Both growth and production are possible in co-culture. To streamline our organism selection process, we started with *T. reesei* as the cellulolytic specialist, greatly reducing the literature search and testing to identify *R. delemar* as an ideal production specialist out of the small number of candidates that satisfied the initial criteria. As indicated in section 3.1.2, we also used *Rhizopus oryzae* to produce lactic acid, which satisfied most of the selection criteria. Unfortunately, we discovered that *T. reesei* could degrade lactic acid at an appreciable rate during our testing.

4.2.2 Analytical techniques for assessing consortia-based CBP performance.

Our earliest co-cultures of *T. reesei* and *R. delemar* were capable of producing fumaric acid. However, productivity was very low compared to the results described in section 3.2.2. Although we could measure the level of glucose and fumaric acid with an HPLC, we did not know how well each organism was actually growing in the culture. We were able to develop a modification of the Updegraff method to quantify the MCC substrate level. However, despite many attempts to quantify the level of each organism, including qPCR of genomic DNA and variations of physical separation, we were not able to achieve a reliable method for quantifying the growth of each organism. This was one of the motivations for the development of selective nitrogen delivery to impose a growth level restriction on each organism, described in section 3.2. In the literature, a number of different methods are used to quantify growth of organisms in co-culture including counting of CFUs, qPCR, gravimetric analysis and physical separation (Balan 2014; Minty et al. 2013; Brethauer and Studer 2014b; Tang, Ou, and Zhu 2015). However, there is little consensus on what constitutes a meaningful measurement of cell growth in mixed cultures. As an alternative, we developed a novel assay for measuring the instantaneous fumaric acid production level of *R. delemar* from a productive consortia (Fig. 3.3B). Our rationale was

that, for productive co-cultures, the activity rate of each organism is more informative than the actual cell growth (especially in long-term cultures where physiology may change drastically).

4.2.3 Compositional control for optimizing consortia performance.

As discussed in section 1.1.2, consortia-based CBP can be more complicated than using a single organism for CBP from a process engineering standpoint. In addition to the requirements for basic compatibility between two or more organisms, there may be a need to control the relative composition of the organisms, especially when they are performing different steps of the same pathway. In our previously unpublished work, we developed selective nitrogen delivery as a mechanism for controlling growth of each organism in the fumaric acid production consortium (Section 3.2).

When it comes to productive microbial cultures where the final product is something besides more cells, there is a fundamental tradeoff between cell growth and production. Many microbial production systems break down over time due to selection against the metabolic burden imposed by production (Wu et al. 2016). In order to avoid this common problem we identified *R. delemar* which naturally separates growth from production. Very efficient production of fumaric acid occurs upon nitrogen limitation, which also ceases growth. For this system, there is a simple tradeoff between production rate, determined by the amount of carbon that goes to growth (number of cells to perform the conversion), and yield, determined by the amount of carbon that goes to product formation. The production rate vs. yield trade off can be tuned by the starting carbon to nitrogen ratio in the culture. This same concept is also true for the consortia system, except that carbon that goes to cell growth is subdivided between two species. Selective nitrogen delivery imposed a limit on the amount of carbon that each species could allocate to cell growth.

This novel mechanism is particularly appealing because it is simple and should be applicable to a variety of systems, even outside of the CBP context. However, selective nitrogen delivery would not be appropriate, or would need to be implemented in a different way, for systems where the product contains nitrogen. The greatest limitation to implementation of this mechanism and other selective delivery systems (eg. carbon) is poorly characterized or changing substrate composition. If the concentration of nitrogen differs between each of a set of substrates (eg. different lignocellulosic biomass substrates), the optimal nitrogen amount and ratio may change. Of course, a set of experiments could still be conducted to determine optimal nitrogen concentration and ratio. Only in cases where the nitrogen introduced by the substrate is close to or exceeds the optimal total nitrogen level would this system totally break down. The other potential problem with engineered selective nitrogen delivery systems may be subject to is imperfect selective delivery. For example, if the rate of acetamide

conversion to ammonia were to greatly exceed the rate of nitrogen utilization for cell growth, the nitrogen could “leak” from one organism and become available to another organism in the same reaction vessel. Although this was not apparent in our selective nitrogen delivery system, this could become a problem for implementation in new systems, especially where growth rate is low.

4.2.4 Outlook on assessing CBP performance and potential of future applications

To our knowledge, there are no industrial-scale consortia-based CBP systems operating commercially. The most research has been devoted to the development of ethanol and butanol as target chemicals for consortia-based CBP (Salehi Jouzani, Jouzani, and Taherzadeh 2015). Although we focus on CBP here, there are operational simultaneous saccharification and fermentation (SSF) systems that rely on the addition of expensive cellulase enzymes that are prepared separately as commercially available cocktails instead of *in situ* enzyme production. As the CBP field progresses, it will likely become increasingly important to establish methods to compare efficiency of CBP systems to commonly used SSF systems. Unfortunately, comparing operating costs of these two systems is not trivial due to input costs and time-scale differences between each operation. In addition to reporting operational parameters for fermentation, such as shaking speed and aeration, which contribute to predictable operational costs, I propose that the current commercial cost or cost projection of cellulase enzyme cocktails also be included in lieu of proprietary enzyme production methods. Some groups have estimated these costs based on available, albeit widely varying, estimates, in which enzyme contributes to a minimum of 5% of the total cost in idealized scenarios (Mielenz 2015; Olson et al. 2012; Biddy et al. 2016)

Although many different platforms for conversion of lignocellulosic biomass into commodity chemicals may be possible, techno-economic analysis will help to identify the most cost-intensive aspects of conversion and thereby allow elimination of the least cost effective routes from research consideration. For example, most microbial production systems are aerobic, which are highly productive, but also more expensive to operate (Wu et al. 2016; Biddy et al. 2016). Clearly, current numbers for these analyses are not abundant or standardized yet. However, transparency about the operational parameters and costs of pricey media components, such as enzyme cocktails and yeast extract, would be beneficial for comparing developmental potential of different production systems.

The major potential benefit of using CBP is the long-term sustainability derived from using lignocellulosic biomass as a feedstock for commodity chemical production in the most consolidated and cost effective manner possible (Laser and Lynd 2014; Lynd et al. 2005). Continuing technological advancements that improve the efficiency and decrease the operating costs could make CBP more

attractive. However, there must also be economic incentive for producing commodity chemicals and biofuels in a sustainable manner as an alternative to the conventional petro-chemical routes (Jang et al. 2012). Uncertainty that this condition will be met in the next decades is probably the single largest factor limiting academic interest and funding for CBP and other research for the utilization of lignocellulosic biomass. Currently there is relatively low public interest in biofuels, the most researched application for CBP, which also coincides with the price of oil. Most likely, a major shift in public support for sustainability and reduction in greenhouse gas emissions will be required for increased funding for research on the utilization of lignocellulosic biomass as a replacement for some oil products. The other major factor that limits the academic and industrial development of CBP is the scale at which CBP could be employed. The scale of CBP is fundamentally constrained by both the availability of lignocellulosic biomass, primarily as farm and forest residues, and the existing infrastructure for efficient transport and conversion of the feedstock (Balan 2014). Although not insurmountable, these are significant problems, given that lignocellulosic biomass a diffuse resource that would require decentralized processing plants. In order for CBP to become economically viable, both the economic environment must change and technological advancements must be made to allow for improved efficiency of conversion.

For chemicals such as fumaric acid, which is currently produced through petrochemical means, there are a limited number of other chemicals which may be used as a replacement (eg. lactic acid for use as a food-acidifier in place of fumaric acid). However, for potential liquid transportation biofuels produced via CBP, there is a direct competition between different portable energy stores including conventional petroleum fuels, emerging lithium-ion battery electric power and other biofuels. Laser and Lynd project that liquid biofuels can compete with electric vehicles in the long term for long-range and heavy-duty operations (Laser and Lynd 2014). One key factor to the economic viability of lignocellulosic biofuels that was included in their analysis was co-production of fuels and other value chemicals. Since lignocellulosic biomass would require significant infrastructure investment to become a widely utilized feedstock, the future impact of CBP may depend on the potential of liquid biofuels to compete with electric powered vehicles (Balan 2014). Therefore, potential CBP systems for the production of non-fuel biochemicals will likely depend not only on their individual markets (commodity chemicals typically have very small margins), but also on the development and profitability of biofuels.

4.3 Concluding remarks and acknowledgements

First, I would like to thank Nina Lin, for giving me a chance in her lab even though I was an unusual student for the Chemical Engineering Department and her first CMB PhD program student. I greatly appreciated the chance to explore my scientific curiosities, a couple of which ended up being fruitful. The respectful lab environment that Nina maintained was valuable for keeping a balance during the sometimes stressful graduate career. In addition, the variety of projects going on in the lab was impressive and taught me many things that I did not expect to learn.

Thank you to Peter Freddolino for first supporting the genome profiling project intellectually and then supporting me as a co-advisor. The genome profiling project always had the same goal, but went through countless iterations of refinement and steps back to fix various problems. It's easy to become frustrated when one has to take steps back to rectify a mistake or oversight from an earlier stage of a project. Peter was always supportive in these situations and also just expected problems to occasionally happen, which helped me keep a balanced perspective on the scale of scientific research. In addition, Peter helped me to broaden my view of the scientific research that we were conducting as a part of large and diverse fields.

I have a six member committee, which is fairly large for a thesis committee. First, thank you to Professors Ken Cadigan, Tom Schmidt, Anuj Kumar and Stephen Ragsdale in addition to my Co-advisors for committing their time to critically thinking about my work. On the one hand, hearing about progress made and scientific success can be fun. On the other hand, I know that every committee member had their own scientific pursuits that they put on hold to think about my questions. I was pleased with the level of scientific and professional rigor that the committee expected. It can be difficult to hear criticism. However, the general committee attitude made it possible to walk into the meeting knowing that criticisms were intended to help me succeed and were raised because the committee thought that these were areas that I could and should improve. These experiences helped me to understand the value of sharing your views in a constructive manner for the good of an individual or team, which I hope to take with me throughout my career.

A special thank you to Ken Cadigan for helping me not only intellectually, but also with the challenges with funding during my graduate career. I hesitate to think about what other paths I might have been forced onto without his help.

A special thank you to Tom Schmidt for first pointing out that ribosomal RNA operons might be involved in the transcriptional propensity peaks that we observed.

Thank you to Professor Bob Fuller: Although he was not directly involved in my projects, I think that Bob knew more about my projects and research situation than could be expected from any

program director. Bob worked tirelessly to promote a strong scientific program for students to succeed in, for which I am extremely grateful. From my time as a student representative on the CMB Program Committee, I can see that directing a diverse program like CMB requires skills that one cannot simply train for.

Many thanks to Pat Ocelnik, Jessica Kijek and Cathy Mitchell, who supported all of the CMB events and students. I read all of your emails even if I was late responding to some of them! Thank you for your personability and professionalism.

Thank you to my peers. Most notably to Rucheng Diao, my collaborator on the genome profiling project. She worked very hard to analyze the deluge of sequencing data while keeping a positive and friendly attitude. Producing and analyzing all of the the high-throughput data was a major team effort. Thank you to Mike Wolfe for creating many useful analysis tools, teaching me what it feels like to get truly destroyed in foosball, and a lot of interesting conversation. Rucheng, Mike and Peter (and Shweta was my personal mentor for my bioinformatics work when I wasn't in lab) also taught me all of the bioinformatics I know, which has already been an extremely useful too. I would like to thank Grace Kroner for many interesting discussions and sharing the burden of writing. I really enjoyed working and talking with Rebecca and Benancio about the pCP20 project and other topics. Thank you to Mehdi for great conversation and fun times, in addition to our hard-fought soccer wins! All of the Freddonlino lab members were very supportive and bright. Special thanks to Tatyana and Adam Krieger of the Lin lab for reading and revising many of my writings. Thank you to David Carruthers for always keeping a respectfully skeptical attitude during meetings etc.. and for teaching me how to/building me a computer! I would also like to acknowledge Elayne Fivenson and Ian Graves, two talented undergraduate research assistants who did everything from fungal culturing to cloning with me. Thank you for your patience. The entire Lin lab has been very supportive of me and tolerant of my views for the past years, for which I am very grateful.

Finally, I would like to thank my friends and family. First, thank you to my great friend and roommate Shweta Ramdas. In addition to having a dangerously sharp wit, Shweta is also extremely supportive. We have been through a lot together over the years at 820 Fuller. We've both grown and changed over that time. I think that I've appreciated her broad worldview and openness to different perspectives the most; not that I didn't appreciate the clever jokes and battle of wills between her + Vroni vs me. I have also greatly benefited from her scientific insight and skill.

Thank you to the entire BIOHAZARDS soccer team. Special thanks to my good friend, discgolf competitor and brewmaster Justin Randall. Special thanks to Adam Krieger and Stephen Beuder, the (at

least) weekly Madras Masala buffet champions and great friends. They have been and continue to be very supportive of me and always have interesting viewpoints on a variety of topics.

Thank you to Vroni Sachsenhauser for supporting me in all things. Sharing my time and life with her has brought perspective and balance that has helped me to become a better person. Aside from being a true companion, her sharp insight and scientific/general skepticism has also been a great influence on me. More importantly, her playful attitude always reminds me of the most important parts of life! There are far too many other things to thank her for to list here!

A huge thanks you to my friends in Oregon: Daniel Gibson - my college roommate and great friend. Tyler Huycke, Mark Leckband, Anthony Maddox, Ashley Lloyd, Anna Maurer, Becky Gibson, Dylan Coleman: The Squad. Wow, I can't thank you guys enough for supporting me through the years. Just knowing that I have such intelligent friends and supportive friends is worth more than anything. It's possible to just go for your dreams if you know that great friends will support you no matter what. Ridiculous friends are a great way to remember that life is for having fun.

Thank you to my ever-supportive parents, Ken and Wendy Scholz. I feel extremely fortunate to have such balanced parents. They have fostered a strong sense of curiosity about the world in us kids. Related to that point, I can see now that they have provided a really great template that we may use, but without any pressure for us to do so. I am proud to have parents that live their lives in such an independent, fun and also morally responsible manner. Thank you to my sister Becky Scholz, who is another sharp scientist that I can call friend. I am very grateful for her scientific input, manuscript editing and support. I know that she will always have an interesting perspective to share that also comes with a strong analytical underpinning for how far a perspective can be applied.

Thank you to my wonderful Grandmothers Jean Scholz and Fujiko Allen. Just knowing how proud they both are of me has helped me to keep working hard and live well. Thank you to Grandma Scholz for her broad perspective on the world and keeping me updated and connected with the rest of the family and Eugene. I don't know what % Grandma's spaghetti I am, but it's significant! Thank you to Grandma Allen for always saying that I am "looking good." In sincerity, many thanks for all of the support and love from my friends and family members that have continually supported me over the years.

Supplementary Figures:

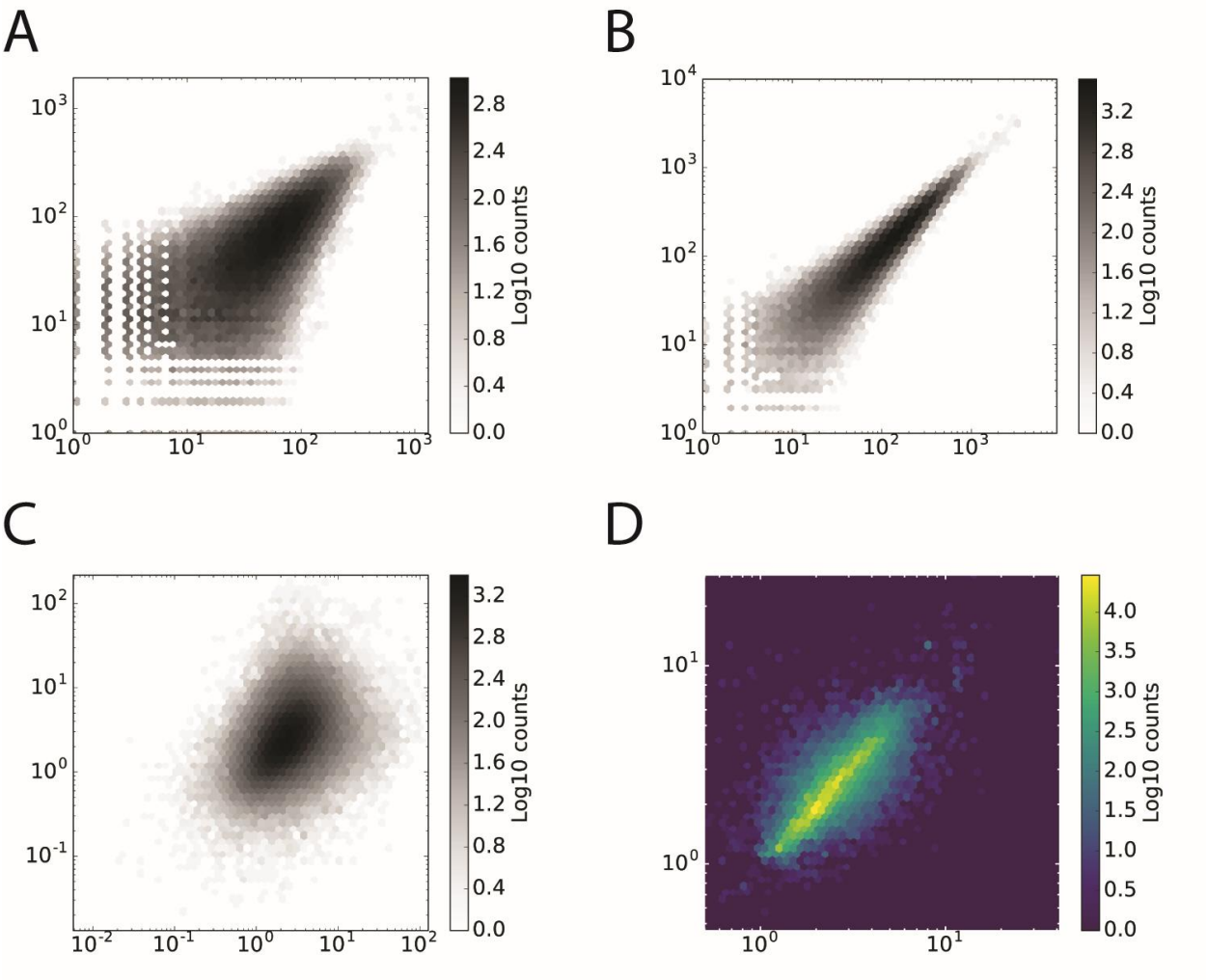

SI Figure 1: Barcode read replicates. A) replicate correlation of DNA barcode counts. (Spearman ρ= 0.72). B) replicate correlation of the RNA barcode counts(Spearman ρ= 0.95). C) replicate correlation of raw RNA/DNA ratios (Spearman ρ= 0.4). D) replicate correlation of DNA RNA/DNA ratios after DNA abundance cutoff (Spearman ρ= 0.91).

Bibliography

Agapakis, Christina M., Patrick M. Boyle, and Pamela A. Silver. 2012. “Natural Strategies for the Spatial Optimization of Metabolism in Synthetic Biology.” *Nature Chemical Biology* 8 (6): 527–35.

Ahamed, Aftab, and Patrick Vermette. 2008. “Culture-Based Strategies to Enhance Cellulase Enzyme Production from Trichoderma Reesei RUT-C30 in Bioreactor Culture Conditions.” *Biochemical Engineering Journal* 40 (3): 399–407.

Akhtar, Waseem, Johann de Jong, Alexey V. Pindyurin, Ludo Pagie, Wouter Meuleman, Jeroen de Ridder, Anton Berns, Lodewyk F. A. Wessels, Maarten van Lohuizen, and Bas van Steensel. 2013. “Chromatin Position Effects Assayed by Thousands of Reporters Integrated in Parallel.” *Cell* 154 (4): 914–27.

Ali Azam, T., A. Iwata, A. Nishimura, S. Ueda, and A. Ishihama. 1999. “Growth Phase-Dependent Variation in Protein Composition of the Escherichia Coli Nucleoid.” *Journal of Bacteriology* 181 (20): 6361–70.

Almario, María P., Luis H. Reyes, and Katy C. Kao. 2013. “Evolutionary Engineering of Saccharomyces Cerevisiae for Enhanced Tolerance to Hydrolysates of Lignocellulosic Biomass.” *Biotechnology and Bioengineering* 110 (10): 2616–23.

Antonov, Elena, Steffen Wirth, Tim Gerlach, Ivan Schlembach, Miriam A. Rosenbaum, Lars Regestein, and Jochen Büchs. 2016. “Efficient Evaluation of Cellulose Digestibility by Trichoderma Reesei Rut-C30 Cultures in Online Monitored Shake Flasks.” *Microbial Cell Factories* 15 (1): 164.

Atlung, T., and H. Ingmer. 1997. “H-NS: A Modulator of Environmentally Regulated Gene Expression.” *Molecular Microbiology* 24 (1): 7–17.

Azam, T. A., and A. Ishihama. 1999. “Twelve Species of the Nucleoid-Associated Protein from Escherichia Coli. Sequence Recognition Specificity and DNA Binding Affinity.” *The Journal of Biological Chemistry* 274 (46): 33105–13.

Baba, Tomoya, Takeshi Ara, Miki Hasegawa, Yuki Takai, Yoshiko Okumura, Miki Baba, Kirill A. Datsenko, Masaru Tomita, Barry L. Wanner, and Hirotada Mori. 2006. “Construction of Escherichia Coli K-12 in-Frame, Single-Gene Knockout Mutants: The Keio Collection.” *Molecular Systems Biology* 2 (February): 2006.0008.

Bakshi, Somenath, Heejun Choi, and James C. Weisshaar. 2015. “The Spatial Biology of Transcription and Translation in Rapidly Growing Escherichia Coli.” *Frontiers in Microbiology* 6 (July): 636.

Balan, Venkatesh. 2014. “Current Challenges in Commercially Producing Biofuels from Lignocellulosic Biomass.” *ISRN Biotechnology* 2014 (May): 463074.

Becker, Nicole A., Jason D. Kahn, and L. James Maher 3rd. 2007. “Effects of Nucleoid Proteins on DNA Repression Loop Formation in Escherichia Coli.” *Nucleic Acids Research* 35 (12): 3988–4000.

Berger, Michael, Veneta Gerganova, Petya Berger, Radu Rapiteanu, Viktoras Lisicovas, and Ulrich Dobrindt. 2016. “Genes on a Wire: The Nucleoid-Associated Protein HU Insulates Transcription

Units in Escherichia Coli." *Scientific Reports* 6 (August): 31512.
Biddy, Mary J., Ryan Davis, David Humbird, Ling Tao, Nancy Dowe, Michael T. Guarnieri, Jeffrey G. Linger, et al. 2016. "The Techno-Economic Basis for Coproduct Manufacturing To Enable Hydrocarbon Fuel Production from Lignocellulosic Biomass." *ACS Sustainable Chemistry & Engineering* 4 (6): 3196–3211.
Blattner, F. R. 1997. "The Complete Genome Sequence of Escherichia Coli K-12." *Science* 277 (5331): 1453–62.
Block, Dena H. S., Razika Hussein, Lusha W. Liang, and Han N. Lim. 2012a. "Regulatory Consequences of Gene Translocation in Bacteria." *Nucleic Acids Research* 40 (18): 8979–92.
Bokal, A. J., 4th, W. Ross, and R. L. Gourse. 1995. "The Transcriptional Activator Protein FIS: DNA Interactions and Cooperative Interactions with RNA Polymerase at the Escherichia Coli rrnB P1 Promoter." *Journal of Molecular Biology* 245 (3): 197–207.
Brambilla, Elisa, and Bianca Sclavi. 2015. "Gene Regulation by H-NS as a Function of Growth Conditions Depends on Chromosomal Position in Escherichia Coli." *G3* 5 (4): 605–14.
Brethauer, Simone, and Michael Hanspeter Studer. 2014a. "Consolidated Bioprocessing of Lignocellulose by a Microbial Consortium." *Energy & Environmental Science* 7 (4): 1446.
Browning, Douglas F., David C. Grainger, and Stephen Jw Busby. 2010. "Effects of Nucleoid-Associated Proteins on Bacterial Chromosome Structure and Gene Expression." *Current Opinion in Microbiology* 13 (6): 773–80.
Broyles, S. S., and D. E. Pettijohn. 1986. "Interaction of the Escherichia Coli HU Protein with DNA. Evidence for Formation of Nucleosome-like Structures with Altered DNA Helical Pitch." *Journal of Molecular Biology* 187 (1): 47–60.
Bryant, Jack A., Laura E. Sellars, Stephen J. W. Busby, and David J. Lee. 2014. "Chromosome Position Effects on Gene Expression in Escherichia Coli K-12." *Nucleic Acids Research* 42 (18): 11383–92.
Cabrera, Julio E., and Ding J. Jin. 2006. "Active Transcription of rRNA Operons Is a Driving Force for the Distribution of RNA Polymerase in Bacteria: Effect of Extrachromosomal Copies of rrnB on the in Vivo Localization of RNA Polymerase." *Journal of Bacteriology* 188 (11): 4007–14.
Caramel, Angela, and Karin Schnetz. 2000. "Antagonistic Control of the Escherichia Coli Bgl Promoter by FIS and CAP in Vitro." *Molecular Microbiology* 36 (1): 85–92.
Carroll, Andrew, and Chris Somerville. 2009. "Cellulosic Biofuels." *Annual Review of Plant Biology* 60 (1): 165–82.
Chai, Qian, Bhupender Singh, Kristin Peisker, Nicole Metzendorf, Xueliang Ge, Santanu Dasgupta, and Suparna Sanyal. 2014. "Organization of Ribosomes and Nucleoids in Escherichia Coli Cells during Growth and in Quiescence." *The Journal of Biological Chemistry* 289 (16): 11342–52.
Chen, Huiyi, Katsuyuki Shiroguchi, Hao Ge, and Xiaoliang Sunney Xie. 2015. "Genome-Wide Study of mRNA Degradation and Transcript Elongation in Escherichia Coli." *Molecular Systems Biology* 11 (5): 808.
Chen, Ying-Ja, Peng Liu, Alec A. K. Nielsen, Jennifer A. N. Brophy, Kevin Clancy, Todd Peterson, and Christopher A. Voigt. 2013. "Characterization of 582 Natural and Synthetic Terminators and Quantification of Their Design Constraints." *Nature Methods* 10 (7): 659–64.
Clavel, Damien, Guillaume Gotthard, David von Stetten, Daniele De Sanctis, Hélène Pasquier, Gerard G. Lambert, Nathan C. Shaner, and Antoine Royant. 2016. "Structural Analysis of the Bright

Monomeric Yellow-Green Fluorescent Protein mNeonGreen Obtained by Directed Evolution." *Acta Crystallographica. Section D, Structural Biology* 72 (Pt 12): 1298–1307.

Dillon, Shane C., and Charles J. Dorman. 2010. "Bacterial Nucleoid-Associated Proteins, Nucleoid Structure and Gene Expression." *Nature Reviews. Microbiology* 8 (3): 185–95.

Ding, Yueyue, Shuang Li, Chang Dou, Yang Yu, and He Huang. 2011. "Production of Fumaric Acid by Rhizopus Oryzae: Role of Carbon-Nitrogen Ratio." *Applied Biochemistry and Biotechnology* 164 (8): 1461–67.

Dolatabadi, Somayeh, G. Sybren de Hoog, Jacques F. Meis, and Grit Walther. 2014. "Species Boundaries and Nomenclature of Rhizopus Arrhizus (syn. R. Oryzae)." *Mycoses* 57 Suppl 3 (December): 108–27.

Dorman, Charles J. 2006. "DNA Supercoiling and Bacterial Gene Expression." *Science Progress* 89 (3): 151–66.

Dunn, Jennifer B., Steffen Mueller, Ho-Young Kwon, and Michael Q. Wang. 2013. "Land-Use Change and Greenhouse Gas Emissions from Corn and Cellulosic Ethanol." *Biotechnology for Biofuels* 6 (1): 51.

Espah Borujeni, Amin, Anirudh S. Channarasappa, and Howard M. Salis. 2014. "Translation Rate Is Controlled by Coupled Trade-Offs between Site Accessibility, Selective RNA Unfolding and Sliding at Upstream Standby Sites." *Nucleic Acids Research* 42 (4): 2646–59.

Fang, Ferric C., and Sylvie Rimsky. 2008. "New Insights into Transcriptional Regulation by H-NS." *Current Opinion in Microbiology* 11 (2): 113–20.

French, S. L., and O. L. Miller Jr. 1989. "Transcription Mapping of the Escherichia Coli Chromosome by Electron Microscopy." *Journal of Bacteriology* 171 (8): 4207–16.

Gaal, Tamas, Benjamin P. Bratton, Patricia Sanchez-Vazquez, Alexander Sliwicki, Kristine Sliwicki, Andrew Vegel, Rachel Pannu, and Richard L. Gourse. 2016a. "Colocalization of Distant Chromosomal Loci in Space in E. Coli : A Bacterial Nucleolus." *Genes & Development* 30 (20): 2272–85.

Gao, Yunfeng, Yong Hwee Foo, Ricksen S. Winardhi, Qingnan Tang, Jie Yan, and Linda J. Kenney. 2017a. "Charged Residues in the H-NS Linker Drive DNA Binding and Gene Silencing in Single Cells." *Proceedings of the National Academy of Sciences* 114 (47): 12560–65.

Girgis, Hany S., Yirchung Liu, William S. Ryu, and Saeed Tavazoie. 2007. "A Comprehensive Genetic Characterization of Bacterial Motility." *PLoS Genetics* 3 (9): 1644–60.

Goyal, Garima, Shen-Long Tsai, Bhawna Madan, Nancy A. DaSilva, and Wilfred Chen. 2011. "Simultaneous Cell Growth and Ethanol Production from Cellulose by an Engineered Yeast Consortium Displaying a Functional Mini-Cellulosome." *Microbial Cell Factories* 10 (November): 89.

Guo, F., and S. Adhya. 2007. "Spiral Structure of Escherichia Coli HU Provides Foundation for DNA Supercoiling." *Proceedings of the National Academy of Sciences* 104 (11): 4309–14.

Haan, Riaan den, Eugéne van Rensburg, Shaunita H. Rose, Johann F. Görgens, and Willem H. van Zyl. 2015. "Progress and Challenges in the Engineering of Non-Cellulolytic Microorganisms for Consolidated Bioprocessing." *Current Opinion in Biotechnology* 33 (June): 32–38.

Hanahan, Douglas, Joel Jessee, and Fredric R. Bloom. 1991. "[4] Plasmid Transformation of Escherichia Coli and Other Bacteria." In *Methods in Enzymology*, 63–113.

Higashi, Koichi, Toru Tobe, Akinori Kanai, Ebru Uyar, Shu Ishikawa, Yutaka Suzuki, Naotake Ogasawara, Ken Kurokawa, and Taku Oshima. 2016. "H-NS Facilitates Sequence Diversification of Horizontally Transferred DNAs during Their Integration in Host Chromosomes." *PLoS Genetics* 12 (1): e1005796.

Hirvonen, C. A., W. Ross, C. E. Wozniak, E. Marasco, J. R. Anthony, S. E. Aiyar, V. H. Newburn, and R. L.

Gourse. 2001. “Contributions of UP Elements and the Transcription Factor FIS to Expression from the Seven Rrn P1 Promoters in Escherichia Coli.” *Journal of Bacteriology* 183 (21): 6305–14.

Jang, Yu-Sin, Byoungjin Kim, Jae Ho Shin, Yong Jun Choi, Sol Choi, Chan Woo Song, Joungmin Lee, Hye Gwon Park, and Sang Yup Lee. 2012. “Bio-Based Production of C2-C6 Platform Chemicals.” *Biotechnology and Bioengineering* 109 (10): 2437–59.

Jeong, Da-Eun, Younju So, Soo-Young Park, Seung-Hwan Park, and Soo-Keun Choi. 2018. “Random Knock-in Expression System for High Yield Production of Heterologous Protein in Bacillus Subtilis.” *Journal of Biotechnology* 266 (January): 50–58.

Jiang, Kai, Ce Zhang, Durgarao Guttula, Fan Liu, Jeroen A. van Kan, Christophe Lavelle, Krzysztof Kubiak, et al. 2015. “Effects of Hfq on the Conformation and Compaction of DNA.” *Nucleic Acids Research* 43 (8): 4332–41.

Jin, Ding Jun, and Julio E. Cabrera. 2006a. “Coupling the Distribution of RNA Polymerase to Global Gene Regulation and the Dynamic Structure of the Bacterial Nucleoid in Escherichia Coli.” *Journal of Structural Biology* 156 (2): 284–91.

Johns, Nathan I., Tomasz Blazejewski, Antonio Lc Gomes, and Harris H. Wang. 2016. “Principles for Designing Synthetic Microbial Communities.” *Current Opinion in Microbiology* 31 (June): 146–53.

Juhász, T., Z. Szengyel, K. Réczey, M. Siika-Aho, and L. Viikari. 2005. “Characterization of Cellulases and Hemicellulases Produced by Trichoderma Reesei on Various Carbon Sources.” *Process Biochemistry* 40 (11): 3519–25.

Kahramanoglou, Christina, Aswin S. N. Seshasayee, Ana I. Prieto, David Ibberson, Sabine Schmidt, Jurgen Zimmermann, Vladimir Benes, Gillian M. Fraser, and Nicholas M. Luscombe. 2011a. “Direct and Indirect Effects of H-NS and Fis on Global Gene Expression Control in Escherichia Coli.” *Nucleic Acids Research* 39 (6): 2073–91.

Kautola, Helena, and Yu-Yen Linko. 1989. “Fumaric Acid Production from Xylose by Immobilized Rhizopus Arrhizus Cells.” *Applied Microbiology and Biotechnology* 31-31 (5-6): 448–52.

Kawaguchi, Hideo, Tomohisa Hasunuma, Chiaki Ogino, and Akihiko Kondo. 2016. “Bioprocessing of Bio-Based Chemicals Produced from Lignocellulosic Feedstocks.” *Current Opinion in Biotechnology* 42 (December): 30–39.

Kerner, Alissa, Jihyang Park, Audra Williams, and Xiaoxia Nina Lin. 2012. “A Programmable Escherichia Coli Consortium via Tunable Symbiosis.” *PloS One* 7 (3): e34032.

Kim, Hyun Jung, James Q. Boedicker, Jang Wook Choi, and Rustem F. Ismagilov. 2008. “Defined Spatial Structure Stabilizes a Synthetic Multispecies Bacterial Community.” *Proceedings of the National Academy of Sciences of the United States of America* 105 (47): 18188–93.

Kim, Sujin, Seung-Ho Baek, Kyusung Lee, and Ji-Sook Hahn. 2013. “Cellulosic Ethanol Production Using a Yeast Consortium Displaying a Minicellulosome and β-Glucosidase.” *Microbial Cell Factories* 12 (February): 14.

Klappenbach, J. A., J. M. Dunbar, and T. M. Schmidt. 2000. “rRNA Operon Copy Number Reflects Ecological Strategies of Bacteria.” *Applied and Environmental Microbiology* 66 (4): 1328–33.

Kosuri, Sriram, Daniel B. Goodman, Guillaume Cambray, Vivek K. Mutalik, Yuan Gao, Adam P. Arkin, Drew Endy, and George M. Church. 2013a. “Composability of Regulatory Sequences Controlling Transcription and Translation in Escherichia Coli.” *Proceedings of the National Academy of Sciences of the United States of America* 110 (34): 14024–29.

Kuhad, Ramesh Chander, Deepa Deswal, Sonia Sharma, Abhishek Bhattacharya, Kavish Kumar Jain, Amandeep Kaur, Brett I. Pletschke, Ajay Singh, and Matti Karp. 2016. “Revisiting Cellulase Production and Redefining Current Strategies Based on Major Challenges.” *Renewable and Sustainable Energy Reviews* 55: 249–72.

Lambertz, Camilla, Megan Garvey, Johannes Klinger, Dirk Heesel, Holger Klose, Rainer Fischer, and Ulrich Commandeur. 2014. “Challenges and Advances in the Heterologous Expression of Cellulolytic Enzymes: A Review.” *Biotechnology for Biofuels* 7 (1): 135.

Lang, Kevin S., Ashley N. Hall, Christopher N. Merrikh, Mark Ragheb, Hannah Tabakh, Alex J. Pollock, Joshua J. Woodward, Julia E. Dreifus, and Houra Merrikh. 2017. “Replication-Transcription Conflicts Generate R-Loops That Orchestrate Bacterial Stress Survival and Pathogenesis.” *Cell* 170 (4): 787–99.e18.

Laser, Mark, and Lee R. Lynd. 2014. “Comparative Efficiency and Driving Range of Light- and Heavy-Duty Vehicles Powered with Biomass Energy Stored in Liquid Fuels or Batteries.” *Proceedings of the National Academy of Sciences* 111 (9): 3360–64.

Le, Tung B. K., Maxim V. Imakaev, Leonid A. Mirny, and Michael T. Laub. 2013a. “High-Resolution Mapping of the Spatial Organization of a Bacterial Chromosome.” *Science* 342 (6159): 731–34.

Le, Tung Bk, and Michael T. Laub. 2016. “Transcription Rate and Transcript Length Drive Formation of Chromosomal Interaction Domain Boundaries.” *The EMBO Journal* 35 (14): 1582–95.

Liao, James C., Luo Mi, Sammy Pontrelli, and Shanshan Luo. 2016. “Fuelling the Future: Microbial Engineering for the Production of Sustainable Biofuels.” *Nature Reviews. Microbiology* 14 (5): 288–304.

Ling, Hua, Weisuong Teo, Binbin Chen, Susanna Su Jan Leong, and Matthew Wook Chang. 2014. “Microbial Tolerance Engineering toward Biochemical Production: From Lignocellulose to Products.” *Current Opinion in Biotechnology* 29 (October): 99–106.

Lioy, Virginia S., Axel Cournac, Martial Marbouty, Stéphane Duigou, Julien Mozziconacci, Olivier Espéli, Frédéric Boccard, and Romain Koszul. 2018a. “Multiscale Structuring of the E. Coli Chromosome by Nucleoid-Associated and Condensin Proteins.” *Cell* 172 (4): 771–83.e18.

Liu, Huan, Weinan Wang, Li Deng, Fang Wang, and Tianwei Tan. 2015. “High Production of Fumaric Acid from Xylose by Newly Selected Strain Rhizopus Arrhizus RH 7-13-9#.” *Bioresource Technology* 186 (June): 348–50.

Lu, Peng, Christine Vogel, Rong Wang, Xin Yao, and Edward M. Marcotte. 2007. “Absolute Protein Expression Profiling Estimates the Relative Contributions of Transcriptional and Translational Regulation.” *Nature Biotechnology* 25 (1): 117–24.

Lynd, Lee R., Willem H. van Zyl, John E. McBride, and Mark Laser. 2005. “Consolidated Bioprocessing of Cellulosic Biomass: An Update.” *Current Opinion in Biotechnology* 16 (5): 577–83.

Madrid, Cristina, Carlos Balsalobre, Jesús García, and Antonio Juárez. 2007. “The Novel Hha/YmoA Family of Nucleoid-Associated Proteins: Use of Structural Mimicry to Modulate the Activity of the H-NS Family of Proteins.” *Molecular Microbiology* 63 (1): 7–14.

Marbouty, Martial, Axel Cournac, Jean-François Flot, Hervé Marie-Nelly, Julien Mozziconacci, and Romain Koszul. 2014. “Metagenomic Chromosome Conformation Capture (meta3C) Unveils the Diversity of Chromosome Organization in Microorganisms.” *eLife* 3 (December): e03318.

Marmann, Andreas, Amal Aly, Wenhan Lin, Bingui Wang, and Peter Proksch. 2014. “Co-Cultivation—A

Powerful Emerging Tool for Enhancing the Chemical Diversity of Microorganisms." *Marine Drugs* 12 (2): 1043–65.

Martínez-Antonio, Agustino, Alejandra Medina-Rivera, and Julio Collado-Vides. 2009a. "Structural and Functional Map of a Bacterial Nucleoid." *Genome Biology* 10 (12): 247.

Mayer, O., L. Rajkowitsch, C. Lorenz, R. Konrat, and R. Schroeder. 2007. "RNA Chaperone Activity and RNA-Binding Properties of the E. Coli Protein StpA." *Nucleic Acids Research* 35 (4): 1257–69.

McNeil, Brian, David Archer, Ioannis Giavasis, and Linda Harvey. 2013. *Microbial Production of Food Ingredients, Enzymes and Nutraceuticals*.

Mielenz, Jonathan R. 2015. "Small-Scale Approaches for Evaluating Biomass Bioconversion for Fuels and Chemicals." In *Bioenergy*, 385–406.

Minty, Jeremy J., Marc E. Singer, Scott A. Scholz, Chang-Hoon Bae, Jung-Ho Ahn, Clifton E. Foster, James C. Liao, and Xiaoxia Nina Lin. 2013. "Design and Characterization of Synthetic Fungal-Bacterial Consortia for Direct Production of Isobutanol from Cellulosic Biomass." *Proceedings of the National Academy of Sciences of the United States of America* 110 (36): 14592–97.

Moreno, Antonio D., David Ibarra, Pablo Alvira, Elia Tomás-Pejó, and Mercedes Ballesteros. 2015. "A Review of Biological Delignification and Detoxification Methods for Lignocellulosic Bioethanol Production." *Critical Reviews in Biotechnology* 35 (3): 342–54.

Nadell, Carey D., Knut Drescher, and Kevin R. Foster. 2016. "Spatial Structure, Cooperation and Competition in Biofilms." *Nature Reviews. Microbiology* 14 (9): 589–600.

Newlands, J. T., C. A. Josaitis, W. Ross, and R. L. Gourse. 1992. "Both Fis-Dependent and Factor-Independent Upstream Activation of the rrnB P1 Promoter Are Face of the Helix Dependent." *Nucleic Acids Research* 20 (4): 719–26.

Nilsson, L., H. Verbeek, E. Vijgenboom, C. van Drunen, A. Vanet, and L. Bosch. 1992. "FIS-Dependent Trans Activation of Stable RNA Operons of Escherichia Coli under Various Growth Conditions." *Journal of Bacteriology* 174 (3): 921–29.

Ninnemann, O., C. Koch, and R. Kahmann. 1992. "The E.coli Fis Promoter Is Subject to Stringent Control and Autoregulation." *The EMBO Journal* 11 (3): 1075–83.

Oberto, Jacques, Sabrina Nabti, Valérie Jooste, Hervé Mignot, and Josette Rouviere-Yaniv. 2009. "The HU Regulon Is Composed of Genes Responding to Anaerobiosis, Acid Stress, High Osmolarity and SOS Induction." *PloS One* 4 (2): e4367.

Olson, Daniel G., John E. McBride, A. Joe Shaw, and Lee R. Lynd. 2012. "Recent Progress in Consolidated Bioprocessing." *Current Opinion in Biotechnology* 23 (3): 396–405.

Parisutham, Vinuselvi, Tae Hyun Kim, and Sung Kuk Lee. 2014. "Feasibilities of Consolidated Bioprocessing Microbes: From Pretreatment to Biofuel Production." *Bioresource Technology* 161 (June): 431–40.

Paul, Brian J., Wilma Ross, Tamas Gaal, and Richard L. Gourse. 2004. "rRNA Transcription in Escherichia Coli." *Annual Review of Genetics* 38: 749–70.

Percival Zhang, Y-H, Michael E. Himmel, and Jonathan R. Mielenz. 2006. "Outlook for Cellulase Improvement: Screening and Selection Strategies." *Biotechnology Advances* 24 (5): 452–81.

Pereira, Francisco B., Miguel C. Teixeira, Nuno P. Mira, Isabel Sá-Correia, and Lucília Domingues. 2014. "Genome-Wide Screening of Saccharomyces Cerevisiae Genes Required to Foster Tolerance towards Industrial Wheat Straw Hydrolysates." *Journal of Industrial Microbiology & Biotechnology*

41 (12): 1753–61.

Price, Morgan N., Eric J. Alm, and Adam P. Arkin. 2005. “Interruptions in Gene Expression Drive Highly Expressed Operons to the Leading Strand of DNA Replication.” *Nucleic Acids Research* 33 (10): 3224–34.

Rainey, F. A., N. L. Ward-Rainey, P. H. Janssen, H. Hippe, and E. Stackebrandt. 1996. “Clostridium Paradoxum DSM 7308T Contains Multiple 16S rRNA Genes with Heterogeneous Intervening Sequences.” *Microbiology* 142 (Pt 8) (August): 2087–95.

Roa Engel, Carol A., Adrie J. J. Straathof, Tiemen W. Zijlmans, Walter M. van Gulik, and Luuk A. M. van der Wielen. 2008. “Fumaric Acid Production by Fermentation.” *Applied Microbiology and Biotechnology* 78 (3): 379–89.

Rocha, Eduardo P. C. 2008. “The Organization of the Bacterial Genome.” *Annual Review of Genetics* 42: 211–33.

Ross, W., J. F. Thompson, J. T. Newlands, and R. L. Gourse. 1990. “E.coli Fis Protein Activates Ribosomal RNA Transcription in Vitro and in Vivo.” *The EMBO Journal* 9 (11): 3733–42.

Salehi Jouzani, Gholamreza, Gholamreza Salehi Jouzani, and Mohammad J. Taherzadeh. 2015. “Advances in Consolidated Bioprocessing Systems for Bioethanol and Butanol Production from Biomass: A Comprehensive Review.” *Biofuel Research Journal*, 152–95.

Schneider, Robert, Andrew Travers, and Georgi Muskhelishvili. 1997. “FIS Modulates Growth Phase-Dependent Topological Transitions of DNA inEscherichia Coli.” *Molecular Microbiology* 26 (03): 519–30.

Schneider, R., A. Travers, T. Kutateladze, and G. Muskhelishvili. 1999. “A DNA Architectural Protein Couples Cellular Physiology and DNA Topology in Escherichia Coli.” *Molecular Microbiology* 34 (5): 953–64.

Scholz, Scott A., Ian Graves, Jeremy J. Minty, and Xiaoxia N. Lin. 2018. “Production of Cellulosic Organic Acids via Synthetic Fungal Consortia.” *Biotechnology and Bioengineering* 115 (4): 1096–1100.

Schuster, André, Kenneth S. Bruno, James R. Collett, Scott E. Baker, Bernhard Seiboth, Christian P. Kubicek, and Monika Schmoll. 2012. “A Versatile Toolkit for High Throughput Functional Genomics with Trichoderma Reesei.” *Biotechnology for Biofuels* 5 (1): 1.

Speers, Allison M., and Gemma Reguera. 2012. “Consolidated Bioprocessing of AFEX-Pretreated Corn Stover to Ethanol and Hydrogen in a Microbial Electrolysis Cell.” *Environmental Science & Technology* 46 (14): 7875–81.

Takada, A., M. Wachi, A. Kaidow, M. Takamura, and K. Nagai. 1997. “DNA Binding Properties of the Hfq Gene Product of Escherichia Coli.” *Biochemical and Biophysical Research Communications* 236 (3): 576–79.

Tang, H., J. F. Ou, and M. J. Zhu. 2015. “Development of a Quantitative Real-Time PCR Assay for Direct Detection of Growth of Cellulose-Degrading bacteriumClostridium Thermocellumin Lignocellulosic Degradation.” *Journal of Applied Microbiology* 118 (6): 1333–44.

Tsoi, Ryan, Feilun Wu, Carolyn Zhang, Sharon Bewick, David Karig, and Lingchong You. 2018. “Metabolic Division of Labor in Microbial Systems.” *Proceedings of the National Academy of Sciences of the United States of America* 115 (10): 2526–31.

Tupper, A. E., T. A. Owen-Hughes, D. W. Ussery, D. S. Santos, D. J. Ferguson, J. M. Sidebotham, J. C. Hinton, and C. F. Higgins. 1994. “The Chromatin-Associated Protein H-NS Alters DNA Topology in

Vitro." *The EMBO Journal* 13 (1): 258–68.

Ueda, Takeshi, Hiroki Takahashi, Ebru Uyar, Shu Ishikawa, Naotake Ogasawara, and Taku Oshima. 2013. "Functions of the Hha and YdgT Proteins in Transcriptional Silencing by the Nucleoid Proteins, H-NS and StpA, in Escherichia Coli." *DNA Research: An International Journal for Rapid Publication of Reports on Genes and Genomes* 20 (3): 263–71.

Ueguchi, C., and T. Mizuno. 1993. "The Escherichia Coli Nucleoid Protein H-NS Functions Directly as a Transcriptional Repressor." *The EMBO Journal* 12 (3): 1039–46.

Uyar, E., K. Kurokawa, M. Yoshimura, S. Ishikawa, N. Ogasawara, and T. Oshima. 2009a. "Differential Binding Profiles of StpA in Wild-Type and Hns Mutant Cells: A Comparative Analysis of Cooperative Partners by Chromatin Immunoprecipitation-Microarray Analysis." *Journal of Bacteriology* 191 (7): 2388–91.

Immunoprecipitation-Microarray Analysis." *Journal of Bacteriology* 191 (7): 2388–91.

Valkonen, Mari, Merja Penttilä, and Mojca Benčina. 2014. "Intracellular pH Responses in the Industrially Important Fungus Trichoderma Reesei." *Fungal Genetics and Biology: FG & B* 70 (September): 86–93.

Vora, Tiffany, Alison K. Hottes, and Saeed Tavazoie. 2009. "Protein Occupancy Landscape of a Bacterial Genome." *Molecular Cell* 35 (2): 247–53.

Waldsich, C. 2002. "RNA Chaperone StpA Loosens Interactions of the Tertiary Structure in the Td Group I Intron in Vivo." *Genes & Development* 16 (17): 2300–2312.

Wu, Gang, Qiang Yan, J. Andrew Jones, Yinjie J. Tang, Stephen S. Fong, and Mattheos A. G. Koffas. 2016. "Metabolic Burden: Cornerstones in Synthetic Biology and Metabolic Engineering Applications." *Trends in Biotechnology* 34 (8): 652–64.

Yeung, Enoch, Aaron J. Dy, Kyle B. Martin, Andrew H. Ng, Domitilla Del Vecchio, James L. Beck, James J. Collins, and Richard M. Murray. 2017. "Biophysical Constraints Arising from Compositional Context in Synthetic Gene Networks." *Cell Systems* 5 (1): 11–24.e12.

Zuroff, Trevor R., and Wayne R. Curtis. 2012. "Developing Symbiotic Consortia for Lignocellulosic Biofuel Production." *Applied Microbiology and Biotechnology* 93 (4): 1423–35.